UNIVERSITY OF CALIFORNIA

Santa Barbara

Sequencing Technologies in Virology: Advancing Pathogen Detection and Understanding Viral-Host Interactions in Human Retinal Organoids

A dissertation submitted in partial satisfaction of the

requirements for the degree

Doctor of Philosophy

In

Biochemistry and Molecular Biology

by

Zachary David Aralis

Committee in charge:

Professor Kenneth S. Kosik, Chair

Professor Carolina Arias

Professor Dennis O. Clegg

Professor Stuart C. Feinstein

March 2024

The dissertation of Zachary David Aralis is approved.

_____
Stuart C. Feinstein

_____
Dennis O. Clegg

_____
Carolina Arias

_____
Kenneth S. Kosik, Committee Chair

January 2024

Sequencing Technologies in Virology: Advancing Pathogen Detection and Understanding Viral-Host Interactions in Human Retinal Organoids

ACKNOWLEDGEMENTS

I extend my deepest gratitude to my advisor, Dr. Carolina Arias, for her unwavering faith in my abilities and for welcoming me into her lab. Her leadership fostered a lab environment that was not just a place of scientific pursuit but a family. I am profoundly thankful for the trust she placed in me, particularly with the COVID-related projects. I am incredibly grateful to Dr. Ken Kosik for his generous invitation to join his lab following Dr. Arias's departure from academia. His lab's warm reception and inclusive atmosphere played a significant role in my seamless transition and sense of belonging.

Special thanks are due to Dr. Denis Clegg and his team for their indispensable support on the retinal organoid projects. In particular, I would like to acknowledge Mohamed Faynus and Mika Katsura for their readiness to assist whenever needed. I am also indebted to Dr. Stu Feinstein, not only for his valuable insights as a member of my committee but also for his exceptional leadership during the pandemic. His guidance was instrumental in the success of our clinical testing lab, which was crucial in addressing UCSB's urgent needs.

My heartfelt appreciation goes to my colleague, Duncan Proctor, for his collaboration and expertise in Zika virus research, retinal studies, and staining techniques. His contributions were vital to the success of our research. The memories of our Aloha Fridays will always be cherished.

I would like to express my gratitude to all members of the Arias group, especially Kevin Bracket and Guillermo Najarro, for their help and camaraderie throughout these years. I am thankful to Dr. Diego Acosta-Alvear and his lab members,

including Micheal Costella and Franchesca Zappa, for their dependable friendship and exemplifying the essence of scientific excellence.

My sincere thanks to the clinicians and laboratory staff at Marian Hospital, Sansum Clinic, UCSB Student Health, Cottage Hospital, and the Santa Barbara Department of Public Health. Their provision of samples, insightful discussions, and overall support were pivotal to our COVID research. I am particularly grateful to Lynn Fitzgibbons for her crucial work and dedication to the safety of Santa Barbara during the pandemic. Collaborating with her was one of the highlights of my time here in Santa Barbara and I will always strive to be as excellent of a person as she is.

I am grateful for the financial support provided by the University of California Santa Barbara, the University of California Office of the President, the CDC's COVID-NET initiative, and the Cottage Health Research Institute. I appreciate Jen Smith's invaluable support on the sequencing projects at the BNL.

My gratitude extends to Osvaldo Moreno, Adriana Ramirez Negron, Dylan David, and Julia Conrad for their technical assistance in the COVID sequencing project, which played a significant role in safeguarding the Santa Barbara community. I thank my undergraduate researcher, Tessa Chou, for her contributions to our research and for allowing me the rewarding experience of mentoring. Teaching you and watching you grow as a scientist were truly some of the most rewarding experiences I had during graduate school.

I would like to thank Kelli Gaines, my high school chemistry teacher, who always believed in me. Your support helped make me the person I am today. Finally, I must express my unbounded gratitude to my friends, family, and partner for their endless

support and encouragement throughout this journey. Thank you all, from the bottom of my heart.

Curriculum Vitae of Zachary David Aralis

Education

2024	Doctor of Philosophy in Biochemistry and Molecular Biology, University of California, Santa Barbara
2014	Bachelor of Science in Biochemistry, California State University, San Marcos

Research Experience

Ph.D.: **Biochemistry and Molecular Biology; University of California, Santa Barbara**
08/2018 to 2/2024
Advisor: Carolina Arias, PhD

- Developed and validated NGS and qPCR assays for identifying SARS-CoV2 variants in human samples to provide variant monitoring for Santa Barbara County Public Health Department.
- Supported development and validation of a low cost CRISPR based method for detection of SARS-CoV2 in human samples and utilized this assay to detect the onset of a COVID outbreak at UCSB and the broader Santa Barbara population.
- Determined the transcriptional responses in HSV1 and ZIKV infected human Retinal Organoids using scRNA-seq.
- Generation of induced pluripotent stem cell (iPSC)-derived retinal organoids for infection modeling.

Assay Specialist/Lab Manager—University of California, Santa Barbara
08/2020 to 9/2023

- Rapidly founded an emergency CAP/CLIA approved clinical lab at UCSB for testing COVID samples in local community.
- Developed and validated multiple clinical assays for use in the UCSB COVID testing lab.
- Managed a team of clinical laboratory scientists and researchers and oversaw testing of over 100,000 clinical tests.
- Supported engagement with local and national regulatory agencies and oversaw and supported internal and external audits.

Research Associate—ResearchDx – Irvine, CA
12/2016 to 08/2018

- Supervised a team of researchers/clinical technicians in the development and implementation of highly complex clinical assays using NGS, Flow Cytometry, PCR, and ELISA.
- Developed assays to extract and sequence cfDNA/ctDNA from human blood for oncology diagnostics.

- Founded flow cytometry department at ResearchDx, onboarded multiple clinical assays previously unavailable to our company that effectively increasing our clinical toolset for assay development.
- Supported the development of a new GMP facility for testing kit production.
- Lead the development of project proposals, design control plans, and technical white papers that supported internal and external stakeholder decision making.
- Supported development of requisite materials used in FDA submissions.

Sr. Medical Lab Associate—Quest Diagnostics/Q2 Solutions – San Juan Capistrano, CA
04/2015 to 12/2016

- Supported development, qualification and validation of cell based, ELISA and qRT-PCR assays used in vaccine immunology testing.
- Authored and reviewed technical standard operating procedures as well as qualifications/validation reports.

Undergraduate Research Associate—California State University, San Marcos
05/2013 to 05/2014

- Studied the structural characteristics of transmembrane proteins involved with peptide amyloid formation.
- Large scale expression and purification of heat shock protein GroEL as well as enzymatic activity characterization to determine optimal conditions for protein activation.

Publications

- **Aralis**, Z.; Comer, S.; Ansorg, H.; Palmer, C.; Smith, J.; Feinstein, S.C.; Fitzgibbons, L.N.; Arias, C. Efficient Tracing of the SARS-CoV-2 Omicron Variants in Santa Barbara County Using a Rapid Quantitative Reverse Transcription PCR Assay. *Diagnostics* **2022**, *12*, 2805. https://doi.org/10.3390/diagnostics12112805
- **Aralis**, Z.; Rauch, J.N.; Audouard, M.; Valois, E.; Lach, R.S.; Solley, S.; Baxter, N.J.; Kosik, K.S.; Wilson, M.Z.; Acosta-Alvear, D.; et al. CREST, a Cas13-Based, Rugged, Equitable, Scalable Testing (CREST) for SARS-CoV-2 Detection in Patient Samples. *Current Protocols* **2022**, *2*, doi:10.1002/cpz1.385.
- Rauch, J.N.; Valois, E.; Ponce-Rojas, J.C.; **Aralis**, Z.; Lach, R.S.; Zappa, F.; Audouard, M.; Solley, S.C.; Vaidya, C.; Costello, M.; et al. Comparison of Severe Acute Respiratory Syndrome Coronavirus 2 Screening Using Reverse Transcriptase–Quantitative Polymerase Chain Reaction or CRISPR-Based Assays in Asymptomatic College Students. *JAMA Network Open* **2021**, *4*, e2037129, doi:10.1001/jamanetworkopen.2020.37129.

Selected Presentations & Awards

- AMS Clinical Virology Symposium "Efficient Tracing of the SARS-CoV-2 Omicron Variant in Santa Barbara County Using a Rapid Quantitative Reverse Transcription PCR Assay", 04/2022
- BMSE/MCDB Symposium “Characterization of Herpes Simples Virus Type 1 Infection in 3D Retinal Organoids”
- UCI Undergraduate Chemistry Symposium “Conformational Properties of a Peptide Corresponding to the Transmembrane Segment of WZA.”
- Connie Frank Fellowship, October 2019

ABSTRACT

Sequencing Technologies in Virology: Advancing Pathogen Detection and Understanding Viral-Host Interactions in Human Retinal Organoids

By

Zachary David Aralis

In virology, the emergence of sequencing technologies has revolutionized our understanding of viral genetics and epidemiology, marking a significant advancement over traditional methods. These techniques provide deep insights into virus genetics, crucial in addressing the challenges of pathogen detection in public health, such as identifying novel pathogens and monitoring rapid viral mutations that can evade current treatments.

This work highlights the crucial role of sequencing as a tool for studying virology, demonstrated through two distinct research approaches. Firstly, we address the challenge posed by the emergence of the SARS-CoV-2 Omicron variant in 2021, which led to a global surge of cases. To identify the introduction of novel SARS-CoV-2 variants in Santa Barbara County, sequencing data was utilized to develop a quantitative reverse transcription PCR-based assay (RT-qPCR), targeting unique mutations in the Omicron BA.1/BA1.1 and BA.2 genomes. This assay, tested on 270 clinical samples from Santa Barbara County, accurately and quickly detected the presence of Omicron variants, showing complete concordance with whole viral genome sequencing. The study demonstrates that by utilizing sequencing data to develop RT-qPCR assays offer a rapid and cost-effective solution for virus variant-

specific detection, streamlining the identification of Omicron variants in clinical samples.

Secondly, the thesis explores the retinal impact of viral infections, focusing on Zika Virus (ZIKV) and Herpes Simplex Virus 1 (HSV1) interactions with human retinal organoids (ROs) using single-cell RNA sequencing (scRNA-seq). The research reveals that early-stage ROs are broadly susceptible to ZIKV, with a robust upregulation of interferon-stimulated genes and the unfolded protein response, suggesting a dynamic cellular defense. In contrast, HSV1 infection in mature ROs suppresses innate immune responses and reduces transcriptomic diversity, indicating distinct viral pathogenesis mechanisms. These findings, unveiled through scRNA-seq, provide crucial insights into the unique mechanisms of ZIKV and HSV1 in the retina, highlighting the value of retinal organoids in ocular virology research and advancing our understanding of viral pathogenesis in sensory organs.

Together, these studies underscore the versatility and efficacy of sequencing technologies in virological research, from rapid pathogen detection and variant identification to understanding complex interactions in viral pathogenesis, thereby informing public health strategies and potential therapeutic interventions.

TABLE OF CONTENTS

ACKNOWLEDGEMENTS iv

CV of Zach Aralis vii

TABLE OF CONTENTS xii

LIST OF FIGURES xvi

List of Tables xvi

Chapter 1: Introduction 1

Introduction to Sequencing Methods in Virology 1

Fundamentals of DNA Sequencing 2

The Role of Sequencing in Pathogen Detection 4

Challenges in Pathogen Detection in Public Health 4

Sequencing as a Tool for Pathogen Detection 4

SARS-CoV-2 Variant Detection in December 2021; A Primer for Chapter 2 7

Sequencing in Understanding Viral Pathogenesis 9

RNA-Sequencing in Viral Research 9

Advancements with Single-Cell RNA Sequencing in Virology 10

Host-Virus Interactions and Retinal Organoids in ZIKV and HSV1 Infections; A Primer for Chapter 3 11

II. Efficient Tracing of the SARS-CoV-2 Omicron Variants in Santa Barbara County Using a Rapid Quantitative Reverse Transcription PCR Assay 18

A. Abstract 18

B. Introduction 19
Material and methods 23
Primer Design 23
Sample collection and RNA extraction 23
RT-qPCR 24
Data Interpretation 24
Amplicon Library Generation, Next Generation Sequencing, Phylogenetic Analysis 25
Results 26
Discussion 32
Chapter 2: Differential Cellular Responses to ZIKV and HSV1 in Human Retinal Organoids Revealed by Single-Cell RNA Sequencing 35
Abstract 35
Introduction 36
Results 38
Early-Stage Retinal Organoids Are Susceptible and Permissive to ZIKV Infection. 38
scRNA-seq Analysis Reveals ZIKV Infection Across All Cell Types in Retinal Organoids 41
Global Transcriptional Response to ZIKV Infection in Retinal Organoids Reveals Interferon Stimulation and UPR Regulation 44
ZIKV and the UPR 47

Activation of Interferon Response in ZIKV-Infected Retinal Organoids 47
Mature Retinal Organoids Are Susceptible and Permissive to HSV1 Infection. 51
Immune Suppression and Transcriptional Alterations in HSV1 Infected Mature Retinal Organoids 54
HSV1 Infection Trajectory in Retinal Organoids 58
Discussion 60
Understanding ZIKV Dynamics in Early-Stage Retinal Organoids 60
Transcriptional Responses to ZIKV Infection in ROs 60
Activation of UPR and ISR in Response to ZIKV 61
Interferon Response and Its Implications in ZIKV Infection 62
Comparative Analysis with HSV1 Infection in Mature ROs 64
Conclusions 65
Methods 65
Cell Lines and Retinal Organoid Differentiation 65
Virus Propagation and Tittering 67
Pharmacological Inhibition and Interferon Treatments 68
Tissue Sectioning 68
RO Immunohistochemistry 69
scRNA-Seq Library Preparation 69
scRNA-Seq Data Analysis 70
Chapter 4: Conclusions and Future Directions 72

Preventing pandemics through robust screening 72
Spatial sequencing of infected ROs 74
Investigating ZIKV Infection in the Retina through Microglia Co-cultured Organoids 76
HSV1 and retinal infections 78
Testing of HSV1 infected early ROs and Testing of ZIKV infected Mature ROs 79
References 81

LIST OF FIGURES

Figure 1. Primer Positions and Method overview 27

Figure 2. Design timeline and metrics of the Omicron variant-specific RT-qPCR 29

Figure 3. Phylogenetic analysis based on whole-genome sequences of SARS-CoV-2 Omicron variants detected in Santa Barbara County. 31

Figure 4. Daily cases and relative variant proportions in Santa Barbara County 32

Figure 5. Characterization and ZIKV Infection of Early-Stage ROs 40

Figure 6. scRNA-seq Analysis of ZIKV Infection in ROs 44

Figure 7. Transcriptional Responses to ZIKV Infected ROs 46

Figure 8. Interferon Response in ZIKV-Infected Retinal Organoids 50

Figure 9. HSV1 Infection Dynamics in Mature Retinal Organoids with GFP-Fused US11 Protein 53

Figure 10. Transcriptional Landscape and Immune Response Alteration in HSV1-Infected Mature Retinal Organoids 57

Figure 11. HSV1 Infection Trajectory in Retinal Organoids 59

List of Tables

Table 1: Methods for analyzing viral genomes 3

Table 2: Alternative methods to detect viral variants in clinical samples 23

Table 3: Primer sequences used in this study 23

Chapter 1: Introduction

Introduction to Sequencing Methods in Virology

In the rapidly evolving field of virology, sequencing methods have become indispensable tools, revolutionizing our understanding of viral genetics and epidemiology. The advent of these technologies marks a significant leap from traditional virological methods, offering unprecedented insights into the genetic makeup of viruses. This section provides an overview of the journey from basic sequencing techniques to the advanced methods currently in use, underscoring their critical role in contemporary virology research.

The roots of sequencing in virology can be traced back to the latter part of the 20th century, with the development of the first sequencing techniques[1]. These early methods, though groundbreaking for their time, were limited by their low throughput, high cost, and labor-intensive nature. However, they laid the foundation for the development of more sophisticated sequencing technologies.

The turn of the millennium witnessed a paradigm shift with the introduction of next-generation sequencing (NGS)[2]. This technology, characterized by its high-throughput capability, allowed for the sequencing of entire viral genomes rapidly and cost-effectively. NGS has not only streamlined the process of viral identification but also enhanced our ability to track viral mutations and understand their implications. The detailed genetic information provided by NGS plays a crucial role in identifying

viral strains, understanding their evolution, and monitoring their spread across populations[3,4].

The impact of these advanced sequencing technologies extends beyond academic research. They are pivotal in clinical virology, aiding in the rapid diagnosis of viral infections and informing public health responses to outbreaks. For instance, the recent COVID-19 pandemic highlighted the significance of sequencing in identifying and tracking the spread of SARS-CoV-2 variants globally[5].

Fundamentals of DNA Sequencing

DNA sequencing technologies are crucial in virological research, offering various methods for analyzing viral genomes with distinct advantages and limitations (Table 1: Methods for analyzing viral (Table 1).

- **Sanger Sequencing**: A classical method developed in 1977, known for its accuracy, but with low throughput and higher per-base cost, limiting its use to specific genomic regions or targeted gene studies.
- **Illumina Sequencing**: This next-generation sequencing (NGS) technique offers high throughput and cost-effectiveness, ideal for whole-genome profiling, despite some limitations like errors in homopolymeric regions[6].
- **SMRT Sequencing (Pacific Biosciences)**: Provides long-read sequencing, useful for de novo genome assembly and complex structures, but with a higher error rate and increased per-base cost[7,8].
- **Oxford Nanopore Sequencing**: Known for its portability and long reads, this method is versatile but has a higher error rate, requiring validation for some applications[9].

Each technology caters to specific virological study needs, with Sanger sequencing excelling in accuracy, Illumina in high-throughput whole-genome profiling, and SMRT and Nanopore in long-read sequencing for complex genomic landscapes[10]. Advances in sequencing technologies continue to enhance the precision and scope of these techniques in virology.

Sequencing Technology	Method Description	Key Features	Advantages	Limitations	Ideal Applications
Sanger Sequencing	Chain-termination method using dNTPs and fluorescently labeled ddNTPs. Electrophoretic separation of terminated sequences.	Exceptional accuracy; Read lengths up to 1,000 bp; Error rate <0.001%.	High accuracy; Long read lengths.	Low throughput; Higher per-base cost.	Validation of specific genomic regions; Targeted gene studies.
Illumina Sequencing	Sequencing-by-synthesis (SBS) approach. DNA templates are attached to a solid surface, amplified, and incorporated with fluorescent dNTPs.	High throughput; Generates millions of short reads (50-300 bp); Cost-effective.	Parallel sequencing of many samples; Short-read accuracy.	Errors in homopolymeric regions; Reduced accuracy in GC/AT-rich areas.	Whole-genome profiling; Large-scale sequencing projects.
SMRT Sequencing (Pacific Biosciences)	Real-time observation of DNA polymerase activity in zero-mode waveguides (ZMWs).	Long reads (10,000-60,000 bp); Real-time sequencing.	Resolves complex structures; De novo genome assembly.	Higher error rate (~1%); Increased per-base cost.	Resolving repeats and transposons ; Complex genomic structures.
Oxford Nanopore Sequencing	DNA strands threaded through protein nanopores; Ionic current changes recorded as DNA translocates.	Portable; Ultra-long reads (>2 Mb); Versatile.	Mobility; Ability to sequence extremely long reads.	Higher error rate (5-15%); Requires validation for certain applications.	On-site sequencing; Studies requiring ultra-long reads.

Table 1: Methods for analyzing viral genomes.

The Role of Sequencing in Pathogen Detection

Challenges in Pathogen Detection in Public Health

Pathogen detection in public health faces several key challenges. Firstly, identifying novel pathogens is difficult due to their unique characteristics and lack of historical data, often leading to misdiagnosis due to non-specific symptoms[11–13]. Secondly, pathogens, particularly viruses, mutate rapidly, creating new strains that may evade current treatments and vaccines. This necessitates continuous genetic monitoring to track pathogen evolution and inform public health strategies.

Another challenge is the speed of diagnostic development. Quick and scalable diagnostic methods are crucial for effective outbreak management but are often not developed rapidly enough to keep pace with emerging threats. These diagnostics must also be accessible in resource-limited settings.[12,13]

The global health impact of these challenges is significant. Delays or inaccuracies in pathogen detection can overwhelm healthcare systems and affect public health policies, such as quarantine measures and vaccine distribution. Therefore, advanced technologies like sequencing have become vital for their ability to rapidly identify unknown pathogens, monitor genetic changes, and provide detailed epidemiological data, thus enhancing public health responses to infectious diseases.

Sequencing as a Tool for Pathogen Detection

Sequencing has become an essential tool in pathogen detection, offering rapid identification and detailed genetic analysis of pathogens. Its ability to quickly identify

unknown pathogens was crucial in the 2014 Ebola outbreak in West Africa, where sequencing helped in the prompt recognition of the Ebola virus, aiding containment and treatment strategies[13].

The ability of sequencing technology to quickly identify unknown pathogens, especially in the context of novel or rapidly mutating viruses and bacteria, was notably demonstrated during the outbreak of Severe Acute Respiratory Syndrome (SARS) in 2003[14]. Traditional methods such as culture and immunoassays were initially unsuccessful in identifying the causative agent. However, the use of sequencing enabled researchers to rapidly identify the novel coronavirus (SARS-CoV) responsible for the outbreak, a task that would have been significantly more challenging with conventional diagnostic methods.

Sequencing enables the monitoring of genetic changes in pathogens, crucial for understanding the evolution of viruses such as influenza or SARS-CoV-2, which is directly linked to vaccine development and treatment effectiveness. For instance, during the COVID-19 pandemic, sequencing rapidly identified and tracked mutations in SARS-CoV-2, such as the Delta and Omicron variants, providing essential information for vaccine development and public health policies[15].

One of the key strengths of sequencing is its high sensitivity, allowing for the detection of pathogens in samples where they are present in low abundance. This is particularly beneficial during the early stages of infection or in cases with low viral load. This feature was demonstrated in early HIV infections, where sequencing facilitated detection and treatment initiation[16,17].

Additionally, the specificity of sequencing aids in accurately distinguishing between closely related pathogens, reducing the likelihood of misdiagnosis. Its specificity also plays a crucial role in accurately distinguishing between closely related pathogens, as seen in differentiating drug-resistant and sensitive strains of Mycobacterium tuberculosis, guiding effective treatment plans[18].

Sequencing provides more than just pathogen detection; it offers a comprehensive profile of the pathogen's genome. This information is invaluable for understanding various aspects of the pathogen, including its transmission dynamics, virulence factors, and mechanisms of drug resistance. During the 2009 H1N1 influenza outbreak, sequencing provided valuable insights into the virus's transmission dynamics and virulence, critical for vaccine development and outbreak management[19].

Furthermore, sequencing plays a critical role in public health surveillance. It aids in tracking the spread and evolution of infectious diseases by analyzing genetic data from various regions and populations, thereby guiding public health responses and control measures. In public health surveillance, sequencing has been instrumental in global poliovirus monitoring, informing vaccination strategies for eradication efforts[20].

The technology is also highly adaptable and scalable. Advances in sequencing have led to the development of customizable assays that can target specific pathogens or a range of potential agents, making it a versatile solution for both localized outbreaks and global pandemic surveillance. This adaptability was crucial during the Zika virus outbreak, where sequencing was rapidly adapted to develop

diagnostic tests, especially for monitoring pregnant women due to the virus's association with birth defects[21]. In summary, the application of sequencing in pathogen detection marks a significant leap forward in infectious disease diagnostics and epidemiology, providing a powerful tool for disease management and public health preparedness.

SARS-CoV-2 Variant Detection in December 2021; A Primer for Chapter 2

In December 2021, the global landscape of the COVID-19 pandemic encountered a significant shift with the arrival of the SARS-CoV-2 Omicron variant. This new variant, distinguished by a host of mutations, particularly in the spike protein, presented challenges distinct from previous variants. Its emergence was not just a testament to the virus's capacity for rapid evolution but also a critical juncture in the pandemic's management. The Omicron variant was marked by increased transmissibility and potential immune evasion, raising concerns worldwide and necessitating an urgent response from the scientific and medical communities[22–28].

At that time, sequencing information was crucial in tracking the evolution of SARS-CoV-2. Labs across the globe were scrambling to scale up their capacity for sequencing viral genomes, to provide needed data on the mutations and spreading patterns of different variants. This genomic surveillance would play a crucial role in understanding the virus's behavior, aiding in the development of vaccines and therapeutic strategies. Despite its importance, the utility of sequencing in real-time pathogen detection faced significant limitations. First, the process was time-intensive and resource-heavy, making it challenging to use sequencing as a standalone tool

for rapid, widespread variant detection in clinical settings. This issue was further exasperated by the fact that the global capacity for sequencing was relatively low in December 2021[29]. This gap was particularly pronounced in the context of the rapidly spreading Omicron variant, where timely identification was crucial for effective public health responses. The turnaround time for sequencing via the state sponsored sequencing initiative was on the order of weeks, if not longer[29]. To address these challenges, our group initiated a local sequencing effort in Santa Barbara County, aiming to provide variant-specific information to our community.

This sequencing data was instrumental in developing rapid, variant-specific diagnostic tests needed to address the limitations of current sequencing turnaround time. Insights gained from sequencing the Omicron variant informed the design of targeted assays. These tests, like the quantitative reverse transcription PCR (RT-qPCR) assays discussed in Chapter 2, were tailored to detect specific mutations of Omicron, offering a much-needed solution for rapid and precise variant identification. This development marked a significant advancement in diagnostic capabilities of our local community, allowing for faster and more efficient tracking of the virus's spread and informing public health decisions.

Chapter 2 of this thesis outlines how the blend of detailed genomic knowledge and practical diagnostic tool development led to the creation of a specific RT-qPCR assay for Omicron, highlighting the synergy between advanced sequencing and rapid diagnostic technologies. This case study exemplifies the dynamic nature of pandemic response, where scientific innovation swiftly adapts to emerging challenges posed by evolving pathogens.

Sequencing in Understanding Viral Pathogenesis

Viral pathogenesis encompasses the complex mechanisms through which viruses invade and affect host cells, leading to disease. It involves multiple stages: virus entry into the host, replication, and spread within the host organism, and the resulting clinical effects[30]. Understanding these mechanisms is critical to virology and medical research, as it informs vaccine development, therapeutic interventions, and public health strategies. Studying viral pathogenesis also contributes to broader scientific knowledge, enhancing our grasp of cellular processes and immune responses.

Sequencing technologies, particularly RNA sequencing (RNA-seq) and its derivative, single-cell RNA sequencing (scRNA-seq), play a pivotal role in modern virology[31–35]. These methods enable detailed analysis of both viral genomes and host responses at single cell resolution. Through sequencing, researchers can better understand the complex interplay between viruses and host cells and unravel the mechanisms behind viral infection and replication. This genomic insight is invaluable in developing effective strategies for controlling and treating viral diseases.

RNA-Sequencing in Viral Research

RNA-sequencing (RNA-seq) has revolutionized virology, offering profound insights into both viral and host genomics. This technique has been pivotal in advancing our understanding of viral behavior and interaction with hosts. A critical application of RNA-seq was evident during the early stages of the COVID-19 pandemic. The technique was instrumental in quickly identifying the genomic sequence of SARS-CoV-2, facilitating rapid global response efforts. Similarly, RNA-

seq has been essential in understanding complex viral replication mechanisms, such as those observed in HIV[36].

Beyond identifying and analyzing viral genomes, RNA-seq offers a window into the host's response to infections. For instance, studies on Hepatitis C Virus (HCV) utilized RNA-seq to explore the host’s transcriptomic response, revealing intricate virus-host dynamics[37]. This understanding is crucial for developing effective treatments and vaccines, as demonstrated in Ebola virus research[13,38]. Moreover, RNA-seq aids in tracking viral evolution and strain diversity, which is particularly vital for rapidly mutating viruses like influenza. Research has shown how RNA-seq can monitor influenza virus evolution, contributing to vaccine development strategies[39–41]. Collectively, these applications highlight RNA-seq's versatility and its crucial role in virology, shaping our response to both existing and emerging viral threats.

Advancements with Single-Cell RNA Sequencing in Virology

Single-cell RNA sequencing (scRNA-seq) has emerged as a transformative tool in virology, enabling an unprecedented understanding of viral infections at the cellular level. This technique allows for the dissection of host responses to viral infection with remarkable precision, revealing the dynamics of virus-host interactions.

A primary application of scRNA-seq is deciphering cell-type-specific reactions to viral infections, revealing how different cells respond variably to the same virus[42–44]. This method has uncovered unexpected cellular or tissue targets of viruses, enhancing our understanding of how viruses function within hosts[45,46]. Additionally, scRNA-seq is crucial in tracing viral replication stages within individual

cells, offering insights into the viral life cycle and HSV1 replication processes at the cellular level[47]. In host-virus interaction studies, scRNA-seq has been pivotal for analyzing individual immune responses to viruses[48]. scRNA-seq data are also essential for developing vaccines and therapeutic strategies, influencing the design of effective interventions against viral diseases[49,50]. As a vital tool in virology, scRNA-seq's detailed infection analysis is transforming our comprehension of viral pathogenesis and driving advancements in targeted treatments and vaccines.

Host-Virus Interactions and Retinal Organoids in ZIKV and HSV1 Infections; A Primer for Chapter 3

The intricate study of host-virus interactions forms a fundamental pillar of virology, delving into the complexities of how viruses infect, replicate, and interact with host organisms. At the heart of these interactions lies the process of viral entry, where viruses specifically attach to receptors on host cells, dictating their range and tissue targeting. Once a virus enters the cell, it commandeers the cellular machinery to replicate its genetic material, a process that varies significantly across different viral types[30].

When a virus invades a host, the innate immune system is the first line of defense. For instance, upon influenza virus infection, cells recognize viral RNA through pattern recognition receptors like RIG-I, leading to the production of interferons[51]. These interferons then activate a cascade of immune responses, including the upregulation of antiviral genes. Additionally, immune cells are mobilized, which can recognize and kill virus-infected cells. For example, NK cells

are known to play a crucial role in controlling herpes simplex virus infections by targeting cells that express stress-induced ligands[52].

Following the initial innate response, the adaptive immune system generates a more specific attack. Antibodies are produced by B cells, which can neutralize viruses like HIV by binding to their surface proteins, preventing them from entering host cells. T cells, on the other hand, target and kill infected cells. In the case of hepatitis B virus (HBV) infection, cytotoxic T lymphocytes target infected hepatocytes and clear the virus[53].

However, viruses are not passive in this interaction. They have evolved sophisticated mechanisms to evade and suppress the host's immune defenses. Some viruses, like HIV, mutate rapidly, changing their surface proteins (antigenic drift) to evade recognition by antibodies[54]. This is why developing an effective vaccine against HIV has been challenging. Viruses like the human papillomavirus (HPV) can interfere with the host's apoptotic machinery. HPV produces proteins (E6 and E7) that bind to and inactivate tumor suppressor proteins p53 and retinoblastoma protein (pRb), respectively, preventing the infected cell from undergoing apoptosis[55]. Viruses can develop resistance to antiviral drugs, which is a significant challenge in treatment. For instance, influenza virus can acquire mutations in its neuraminidase protein, rendering neuraminidase inhibitors less effective[56].

Viral infections in the retina, an immune privileged tissue, represent a critical area of study due to the retina's essential role in vision and its susceptibility to various viral pathogens. The retina, a layer of tissue at the back of the eye, is responsible for

receiving light and converting it into neural signals for the brain[57]. Viruses can reach the retina through different routes, including hematogenous spread or direct extension from neighboring structures, leading to retinal infections[58–61].

The consequences of viral infections in the retina can be severe, ranging from mild inflammations to severe conditions that can cause permanent vision loss[62]. Common manifestations include retinitis, choroiditis, and vasculitis, each presenting unique clinical features and challenges in management. Retinitis, for instance, often results in the deterioration of the light-sensitive layer of cells in the retina, leading to visual impairment[63].

The human retina is vulnerable to a variety of viruses, each with distinct mechanisms of infection and pathogenesis. For example, cytomegalovirus (CMV) retinitis is one of the most common ocular complications in immunocompromised individuals, particularly in patients with AIDS[59]. Herpesviruses, such as Varicella-zoster virus and Herpes Simplex virus, can also cause acute retinal necrosis, characterized by rapid, progressive inflammation and necrosis of the retina[64,65].

The study of viral infections in the retina is not only important for understanding and managing these specific conditions but also for gaining insights into broader mechanisms of viral pathogenesis and host defense. Understanding the complex interactions between viruses and retinal cells is crucial for developing more effective treatments and preventive strategies for retinal viral infections.

Zika virus (ZIKV), a member of the Flaviviridae family, has emerged as a significant public health concern, particularly due to its association with congenital abnormalities and neurological complications[66]. ZIKV is primarily transmitted to

humans through the bite of an infected Aedes species mosquito, but it can also be transmitted through sexual contact, blood transfusion, and from mother to child during pregnancy.

The connection between ZIKV infection and retinal damage became evident following the 2015 outbreak in Brazil, where an increase in cases of microcephaly and other congenital abnormalities in infants was observed[67,68]. These congenital anomalies included ocular abnormalities, with ZIKV being identified in the retinal tissues of affected infants[67]. The virus has been shown to target retinal cells, potentially leading to a range of ocular complications such as chorioretinal atrophy, optic nerve abnormalities, and maculopathy[69]. The specific mechanisms by which ZIKV causes retinal damage are not yet fully understood, but research suggests that the virus may disrupt the development and function of retinal cells, leading to visual impairment[66]. Given the potential for severe and irreversible ocular damage, understanding the interaction between ZIKV and retinal cells is crucial.

Herpes Simplex Virus 1 (HSV1), a prevalent pathogen within the human population, is known for its ability to establish latent infections in nerve cells and cause recurrent diseases[70]. HSV1, a member of the Herpesviridae family, primarily infects epithelial cells and then establishes latency in sensory neurons[71]. It can reactivate periodically, leading to symptomatic or asymptomatic viral shedding.

HSV1 infection in the retina manifests as Herpes Simplex Retinitis (HSR), which can be a severe and potentially blinding condition[62]. HSR often presents as acute retinal necrosis, characterized by rapid, progressive inflammation and necrosis of the retina, leading to vision loss if not promptly and effectively treated. The virus can

affect various retinal cell types, causing a range of pathological changes, including retinal detachment, hemorrhage, and optic atrophy.

The pathogenesis of HSV1 in the retina involves both direct viral cytotoxic effects and immune-mediated damage. During reactivation, the virus travels from the sensory ganglia back to the ocular tissues, causing inflammation and cell death. The immune response to the virus, while necessary to control the infection, can also contribute to tissue damage due to the release of inflammatory cytokines and recruitment of immune cells[70,72–74]. Understanding ZIKV and HSV1's interaction with retinal cells is crucial for developing effective treatments and preventative strategies for retinal diseases caused by this virus.

In the infections of sensory organs like the retina, significant questions remain unanswered. These questions often revolve around the mechanisms of viral entry, replication, and pathogenesis in specific cell types within the retina, as well as the interplay between the virus and the host's immune response. These unanswered questions highlight the complex interplay between viral pathogenesis and host responses in the retina. They underscore the need for advanced research tools and models to study these interactions in a more detailed and physiologically relevant manner.

The application of retinal organoids in virological research offers a transformative approach for studying viral infections in the retina. Simal organoid models have been used to study ZIKV and HSV1 infections in the brain. Retinal organoids are three-dimensional (3D) structures derived from human pluripotent stem cells (hPSCs) that closely mimic the cellular architecture and physiology of the human retina. This

innovative model overcomes many limitations of traditional two-dimensional (2D) cell culture systems and animal models, providing a more accurate representation of human retinal development and disease.

Retinal organoids have several key advantages for studying viral pathogenesis in the retina. First, they replicate the complex, multi-layered structure of the retina, including various cell types such as photoreceptors, retinal ganglion cells, and Müller glia[75,76]. This diversity allows for a comprehensive investigation of how different viruses interact with and affect specific cell types in the retina. Additionally, these organoids can be used to model both early developmental stages and mature retinal structures, making them suitable for studying infections that occur during different stages of retinal development. Retinal organoids have been used to study a number of other pathologies including SARS-CoV-2, Retinitis pigmentosa, inherited retinal dystrophies, age-related macular degeneration [77–80].

Furthermore, retinal organoids are valuable for screening potential antiviral drugs and therapies. They provide a physiologically relevant platform to test the efficacy and safety of new treatments for viral infections of the retina, potentially accelerating the development of targeted therapies[81].

The use of retinal organoids in this study is aimed at advancing our understanding of ZIKV and HSV1 infections in the retina. By employing these organoids, we can explore the cellular and molecular dynamics of these infections with greater precision and relevance to human pathology. This approach promises to unveil critical insights into the mechanisms of viral pathogenesis in the retina and to guide the development of effective strategies for prevention and treatment.

Chapter 3 of this thesis highlights the susceptibility and permissiveness of early-stage retinal organoids (ROs) to Zika Virus (ZIKV) infection. We demonstrate that ZIKV can infect a broad spectrum of cell types in immature ROs, mimicking the developmental stage of the embryonic retina. The transcriptional responses to ZIKV infection in ROs, as revealed by scRNA-seq, show that ZIKV affects various cellular pathways, including the interferon system and Unfolded Protein Response (UPR), significantly altering the cellular transcriptome. In contrast, HSV1 displays a different interaction pattern, marked by suppression of the innate immune response and a loss of cellular identity in infected cells. This contrast between ZIKV and HSV1 infections underscores the specificity of viral strategies in modulating host responses and emphasizes the complexity of viral interactions with host cells. The chapter underscores the utility of retinal organoids as a comprehensive model for studying ocular viral infections.

II. Efficient Tracing of the SARS-CoV-2 Omicron Variants in Santa Barbara County Using a Rapid Quantitative Reverse Transcription PCR Assay

A. Abstract

The emergence of the SARS-CoV-2 Omicron variant in 2021 is associated with a global surge of cases in late 2021 and early 2022. Identifying the introduction of novel SARS-CoV-2 variants to a population is imperative to inform decisions by clinicians and public health officials. Here, we describe a quantitative reverse transcription PCR-based assay (RT-qPCR) targeting unique mutations in the Omicron BA.1/BA1.1 and BA.2 viral genomes. This assay accurately and precisely detects the presence of these Omicron variants in patient samples in less than four hours. Using this assay, we tested 270 clinical samples and detected the introduction of Omicron BA.1/BA1.1 and BA.2 in the Santa Barbara County (SBC) population in December 2021 and February 2022, respectively. Identifying Omicron variants using this RT-qPCR assay showed complete concordance with whole viral genome sequencing; both assays indicated that Omicron was the dominant variant in SB County. Our data substantiate that RT-qPCR-based virus detection assays offer a fast and inexpensive alternative to NGS for virus variant-specific detection approach, which allows streamlining the detection of Omicron variants in patient samples.

B. Introduction

SARS-CoV-2, the causative agent of the COVID-19 pandemic, is a single strand positive RNA virus of the coronavirus family. COVID-19 has caused a devastating number of cases and deaths since it was officially declared a pandemic on March 11th, 2020. Despite the development of successful vaccines and global vaccination efforts, SARS-CoV-2 continues to spread globally[82–84]. A challenge in controlling COVID-19 is the emergence of SARS-CoV-2 variants resulting from mutations that accumulate in the viral genome. While many of these mutations are of little to no consequence, others can provide a higher viral fitness by increasing virus transmission efficiency, conferring resistance to immune responses, and impacting the severity of the disease[85–87]. SARS-CoV-2 variants that pose a significant risk to the global community are designated Variants of Concern (VOC) by the World Health Organization (WHO)[88]. The control of SARS-CoV-2 transmission relies on our capacity to diagnose COVID-19 efficiently, detect the emergence of new viral lineages, and determine variant prevalence in the population[89–92].

One of the most infectious SARS-CoV-2 variants identified, Omicron BA.1 (originally B.1.1.529), was initially detected in South Africa in November of 2021, where it rapidly outcompeted other viral variants in the region[93]. In November 2021, the WHO classified SARS-CoV-2 Omicron as a VOC and linked it to a global upsurge of cases at the end of 2021[94]. By December 2021, the highly transmissible Omicron variant had caused more than half of all daily SARS-CoV-2 infections[95]. Omicron carries numerous mutations, including 30 in the Spike (S) protein, which enhance binding to the cellular receptor ACE2 and increase immune

evasion[22–27]. The BA.1.1 sublineage shows all the mutations found in BA.1 and the R346K substitution[96].

The high transmission rates of Omicron forecasted the emergence of sublineages, for example, BA.2, a highly contagious variant first detected in December 2021 and classified as a VOC in February 2022 [97]. While the global prevalence of BA.2 was lower than that of BA.1/BA.1.1 through January and February of 2022, it accounted for over 50% of the cases sequenced by the first week of March. Several mutations in the S protein distinguish BA.2 from BA.1/BA.1.1 and may enhance this variant's transmissibility and immune evasion [97].

The numerous mutations in the S protein in BA.1/BA1.1 and BA.2 limit the options for treatment; of the three monoclonal antibody treatments approved for early use by the FDA, only Sotrovimab is effective against BA.1/BA.1.1 Omicron variant. However, this monoclonal antibody is ineffective in treating the BA.2 Omicron Variant[98]. Even though testing each patient to identify the infecting viral variant and tailor individual treatment is impractical, understanding the prevalence of specific variants in the community can inform decisions about using monoclonal antibodies and other COVID-19 therapies.

Next-generation sequencing (NGS) of the viral genome is the standard method to determine the SARS-CoV-2 variants in a sample. While NGS provides a wealth of information on the mutations present in an individual strain of the virus, it typically takes days to weeks to accurately identify viral variants. Rapid and straightforward methods to identify Omicron and other emerging viral variants are urgently needed

to provide clinicians and public health officers with essential real-time information on the prevalence of specific SARS-CoV-2 variants in the population. In response to this emergency, several groups have developed alternative methods to detect viral variants in clinical samples (Table 2).

Here we developed an RT-qPCR-based assay to distinguish between the Omicron BA.1/BA.1.1 and BA.2 variants of SARS-CoV-2 by targeting a set of variant-specific mutations in the S1 domain. We designed variant-specific RT-qPCR primers after homing in on viral genomic regions characterized by significant mutations, insertions, or deletions unique to specific variants. This strategy is versatile and can be easily adapted to identify emerging variants in the population. Using this simple RT-qPCR-based assay in residual diagnostic samples, we identified the BA.1/BA1.1 and BA.2 Omicron variants in patient samples with 100% accuracy compared to sample-matched NGS results. Our assay also provides a rapid, cost-effective alternative for SARS-CoV-2 variant identification; the time from assay design to deployment in patient samples is approximately one week, and its cost is lower than NGS-based approaches. Notably, the development of our assay was informed by the needs of our local public health department and hospitals. By immediately disseminating the results of our assays with health officials and clinicians, we provided vital information to treat active cases in the region and help manage the dramatic rise in COVID-19 cases in Santa Barbara County.

Method	SARS-CoV-2 Variants	Mutations Targeted	Reference
RT-qPCR	Omicron	N:S135R; N:I189V; S:A27S; S:S371L; N:F108L; S:G446S; S:T547K; S:L981F; N:T24I; N:L1266I; S:V213G; S:R408S	Li et al.[99]

RT-qPCR	Omicron	N:31Del; N:32Del; N:33Del; N:P13L; N:R203K; N:G204R	Ippoliti et al.[100]
RT-qPCR	Omicron	S:E484A; S:Y505H	Corbisier et al.[101]
RT-ddPCR	Omicron	S:S477N; S:T478K; S:E484A; S:G496S; S:Q498R; S:N501Y S:Y505H	Mills et al.[102]
High-Resolution Melting analysis	Omicron	S:G339D; S:N440K; S:G446S; S:D796Y	Koshikawa et al.[103]
High-Resolution Melting analysis	BA1.1/BA1.2	S:R408S; S:G446R; S:447N; S:T448K	Aoki et al.[104]
MeltaArray	Alpha, Delta, BA.1, BA.2, BA.3, and BA.4/5	S:A67V; S:T95I; S:Del69/70; S:G142D; S:Del143/145; S:N211I; S:Del212; S:Ins214EPE; S:G339D; S:S371L; S:S373P; S:S375F; S:K417N; S:N440K; S:G446S; S:S477N; S:T478K; S:E484A; S:Q493R; S:G496S; S:Q498R; S:N501Y; S:Y505H; S:T547K; S:D614G; S:H655Y; S:N679K; S:P681H; S:N764K; S:D796Y; S:N856K; S:Q954H; S:N969K; S:L981F;	Yan et al.[105]
Multiplex Fragment Analysis	Delta, Mu, Lambda, Omicron	S:Del69/70; S:Ins146N; S:Del144; S:Del156/157; S:Del143/145; S:Del241/243; S:Ins214EPE; S:Del211; S:Del247/253; S:L452R S:E484K; S:N501Y; ORF1A:Del3675/3677; ORF8:Ins28269/28273; ORF8:Del119/120; ORF8:Del31/33;	Clark et al.[106]
Mass Spectrometry	Iota, Alpha, Delta, and Omicron	S:L5F; S:S13I; S:L18F; S:T19R; S:Del69/70; S:D80A; S:D80G; S:T95I; S:Del144; S:W152C; S:D215G; S:Del242/244; S:D253G; S:K417N; S:K417T; S:N439K; S:L452R; S:Y453F; S:S477N; S:T478K; S:E484Q; S:E484K; S:Q493K; S:N501Y; S:N501T; S:A570D; S:D614G; S:Q677H; S:Q677P; S:P681H; S:P681R; S:I692V;	Hernandez et al.[107]

Table 2: Alternative methods to detect viral variants in clinical samples

Material and methods

Primer Design

The coordinates of all primers and sequences are based on the SARS-CoV-2 Wuhan-Hu-1 (Wu-Hu1) genome (accession number NC_044512.2). The primers for BA.1/BA.1.1 specific targets were designed to target a 3-nucleotide deletion at position 22194-22196 and a 9-nucleotide insertion previously reported for this variant[108,109]. For BA.2, specific primers were designed to target a 9-nucleotide deletion at position 21633–21641 and the lack of a 6-nucleotide deletion at amino acids 69/70 present in BA.1/BA.1.1 and other VOCs[110]. The positions of the primers are illustrated in Figure 1, and the primer sequences are shown in Table 3.

Name	Bases (5' - 3')	Target
S-BA.1/BA.1.1 Fwd	ATTATAGTGCGTGAGCCAGAAGATCT	BA.1/BA.1.1
S-Wu-Hu1 Fwd	ATTAATTTAGTGCGTGATCTCCCT	All Other variants
S-Rev	GCAAGTAAAGTTTGAAACCTAGTGATT	All Variants
S-BA.2 Fwd	tcttataaccagaactcaatcatacact	BA.2
S-BA.2 Rev	ccattggtcccagagacatgta	BA.2

Table 3: Primer sequences used in this study

Sample collection and RNA extraction

Clinical samples were acquired as residual NP swabs stored in Universal Transport Media (UTM) or Viral Transport Media (VTM). Samples were inactivated at 56 °C for 30 minutes, and RNA was extracted using the QIAamp MinElute Virus

Spin Kit [Qiagen, 57704] from 140µL of the sample, and eluted in 50 µL. The Santa Barbara Cottage Hospital IRB reviewed and approved pre-and post-analytical protocols. This study followed the Strengthening the Reporting of Observational Studies in Epidemiology (STROBE) reporting guideline for cohort studies.

RT-qPCR

Viral RNA was reverse transcribed by mixing 8 µL of extracted RNA with 2 µL of LunaScript RT SuperMix [NEB, E3010L], followed by incubation using the thermal profile: 25°C for 2 minutes, 55°C for 10 minutes, and 95°C for 2 minutes. A qPCR master mix was prepared by combining 5 µl of nuclease-free water, 2 µl of 5µM S-Omicron or S-Wu-Hu1 Fwd primer, 2 µl of 5µM S-reverse primer, 10 µl of the PowerUp™ SYBR™ Green Master Mix [Applied Biosystems, A25741], and 1 µL of cDNA, for a total reaction volume of 20 µL. All components were gently mixed by pipetting, and the reactions were collected by centrifugation using a tabletop centrifuge. The reactions were run on a Bio-Rad CFX96 Touch using the following thermal protocol: 50°C for 2 minutes; 95°C for 2 minutes; 40 cycles of 95°C for 15 seconds followed by 60°C for 1 minute, and the plate read in the SYBR/Fam channel. Data were analyzed using the Bio-Rad CFX Maestro software with a single threshold to determine the quantification cycle.

Data Interpretation

The assay was considered valid if the samples had a Ct value equal to or lower than 37 in the reactions with the S-BA.1/BA.1.1, BA.2 or S-Wu-Hu1 reaction. This cutoff is defined as the Ct value below by which virus variants in all samples could

be successfully determined via NGS. Samples were defined as SARS-CoV-2 BA.1/BA.1.1 or BA.2 if the Ct value for the sample was equal to or lower than 37 in the qPCR reaction, including the S-Omicron BA.1/BA.1.1 or BA.2 Fwd primer. In the qPCR reaction, samples with Ct values above 37, including the S-Omicron or S-Wt primers, were deemed inconclusive. In limited cases, a small number of samples with low Ct values for one target had background amplification for one of the other targets, likely caused by non-specific amplification typically observed in mutation-specific qPCR assays[111–113]. In these cases, if the difference between Ct values was greater than 10 Ct, the target with the higher value was not considered (i.e., undetermined).

Amplicon Library Generation, Next Generation Sequencing, Phylogenetic Analysis

Viral cDNA was generated using LunaScript RT SuperMix, followed by incubation using the thermal profile: 25°C for 2 minutes, 55°C for 10 minutes, and 95°C for 2 minutes. The cDNA was amplified using the SARS-CoV-2 genome tiling primer pools from the UCSF CAT COVID-19 Tailed 275bp ARTIC V3 Protocol.[114] The PCR reaction was prepared by mixing 5µL of Q5 Hotstart 2X Master Mix [NEB, M0494S], 1.8µL of primer pool 1 or 2, 2.2µL of nuclease-free water, and 1µL of cDNA per sample. Amplification was carried out at 98°C for 30 seconds, followed by 35 cycles of 95°C for15 seconds and 63°C for 5 minutes. Pools 1 and 2 were combined, diluted 100-fold in nuclease-free water, and indexed using NEBNext dual index oligos for the Illumina [NEB, E6440S]. Equal sample volumes were pooled, cleaned up with AMPureXP beads, and sequenced on a NextSeq 500 instrument

using a NextSeq 500/550 Mid Output Kit v2.5 (300 Cycles) kit. The demultiplexed FASTA files were uploaded to CZ ID for alignment. Consensus sequences were uploaded to Pangolin COVID-19 Lineage Assigner for variant identification. Consensus sequences generated by NGS were uploaded to Nexstrain for phylogenetic analysis[115]. Phylogenetic trees were visualized with the ggtree package in R[116].

Results

The Omicron variant of SARS-CoV-2 initially reported at the end of November 2021 in South Africa, is characterized by numerous mutations throughout the genome. Most of these mutations, 30 in BA.1/BA.1.1 and 20 in BA.2, have been described in the gene encoding the Spike (S) protein gene. To develop a quantitative reverse transcription PCR (RT-qPCR)-based assay to precisely detect the Omicron variant sublineages BA.1/BA.1.1 and BA.2 in clinical samples, we designed primers targeting unique mutations present in the S gene of each of these variants. The BA.1/BA.1.1 primers target the N211 deletion (N211del), the L212I substitution, and the 214 EPE insertion (ins214EPE) (Fig 1A). The BA.2 primers target the T19I substitution and L24/P25/P26 deletion (Fig 1B). In parallel, we designed the S-Wu-Hu1 primer targeting the region in the S gene encoding for amino acids (AA) 210-217 that would recognize all SARS-CoV-2 variants of concern, except for Omicron BA.1/BA.1.1 (Fig 1A). Our RT-qPCR assay takes less than 4 hours from RNA extraction to readout (Fig 1C). We successfully designed and validated the assay and obtained results from patient samples within one week (Fig 2A).

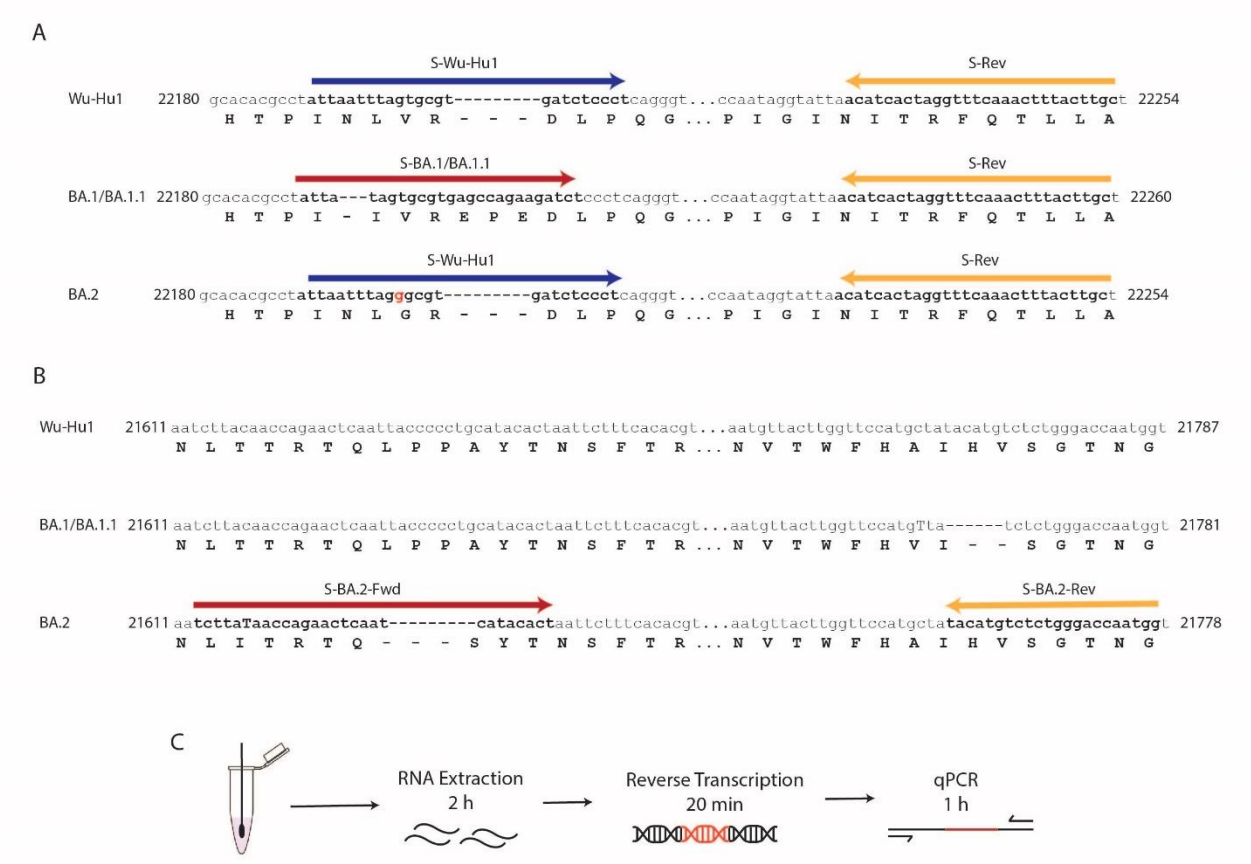

Figure 1. Primer Positions and Method overview. Genomic coordinates of the primer binding locations in the Wu-Hu1, BA.1/BA.1.1, and BA.2 viral variant genomes for (A) the BA.1/BA.1.1 targets and (B) the BA.2 targets. (C) Schematic and estimated timeline of RT-qPCR assay.

To validate this assay, we obtained 270 residual SARS-CoV-2 positive nasopharyngeal swab samples collected for diagnostic purposes between December 2021 and February 2022 with undetermined viral variants (Fig 2A. Timeline). As a control, we used 29 retrospective residual SARS-CoV-2 positive nasopharyngeal swab samples we previously identified by viral genome sequencing as 20B, 20C, Epsilon (CAL.20C), Gamma (P.1), Lambda (C.37), Alpha (B.1.1.7), and Delta (B.1.617.2 and AY) (Fig 2B). Using our RT-qPCR assay in this cohort, we

detected BA.1/BA.1.1 in 164 samples (60.7% of total), BA.2 in 5 samples (1.9% of total), and other variants in 34 samples (12.6% of total). Our results confirmed the overwhelming presence of SARS-CoV-2 Omicron in most samples collected in late 2021/early 2022. The 67 remaining samples failed due to a lack of amplification and detection by RT-qPCR with the S-Omicron or the S-Wu-Hu1 primers, possibly due to low viral load or poor sample preservation (Fig 2D). The control samples previously identified to contain viral RNA for the SARS-CoV-2 variants 20B, 20C, Alpha, Delta, Epsilon, Gamma, and Lambda were all positive by RT-qPCR with the S-Wu-Hu1 but not with the S-Omicron BA.1/BA.1.1 specific primers (Fig 2C).

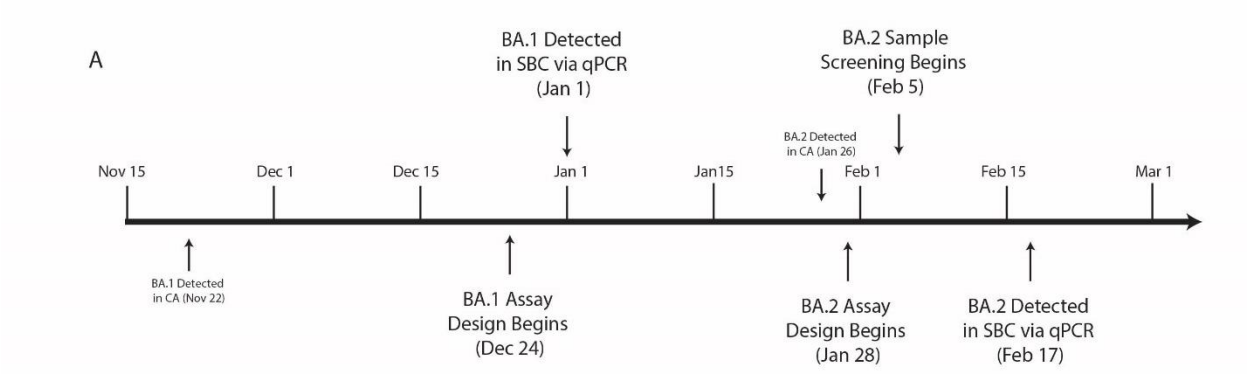

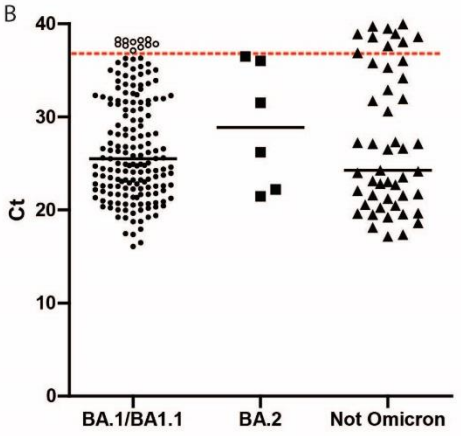

C

	Primer Used in RT-qPCR		
Variant ID	S-BA.1/BA.1.1 (Ct Range)	S-BA.2 (Ct Range)	S-Wu-Hu1 (Ct Range)
20B	ND	ND	22.3-24.2
20C	ND	ND	24.5-30.2
Alpha	ND	ND	20.3-25.1
Delta	ND	ND	18.1-29.6
Epsilon	ND	ND	25.8
Gamma	ND	NT	20.5-27.1
Lambda	ND	NT	24.40

D

	Samples Tested n=270			
	BA.1/BA.1.1	BA.2	Not Omicron	Failed/Invalid
numer of samples	164	5	34	67
% of samples	60.7	1.9	12.6	24.8

E

	Samples Sequenced n = 124			
	BA.1/BA.1.1	BA.2	Not Omicron	Failed
Number	83	5	3	33
% of total	66.9	4.0	2.4	26.6
% Concordance	100	100.0	100.0	100

F

		Predicted			
		BA.1/BA.1.1	BA.2	Not Omicron	
Actual	BA.1/BA.1.1	83	0	0	Sensitivity 100%
	BA.2	0	5	0	
	Not Omicron	0	0	32	
		Precision 100%			Accuracy 100%

Figure 2. Design timeline and metrics of the Omicron variant-specific RT-qPCR. (A) Timeline of events around the design, optimization, and implementation of the Omicron variant-specific RT-qPCR in Santa Barbara County. (B) Ct values for all samples tested. The red dashed line indicates the cutoff at a Ct of 37. (C) Ct values of a panel of samples known to be variants other than Omicron BA.1, BA.1.1, and BA.2. (D) Results of all 270 samples

tested. (E) Percent concordance and (F) confusion matrix of samples with whole viral NGS and variant-specific RT-qPCR data. ND: not detected; NT: not tested.

To confirm the presence of the Omicron variant in these clinical specimens and evaluate the accuracy of our assay, we sequenced the viral genome in 124 of the 270 patient samples that were tested using our RT-qPCR assay. We identified 83 SARS-CoV-2 Omicron BA.1/BA.1.1 (91.2% of samples successfully sequenced), 5 Omicron BA.2 (5.5%), and 3 SARS-CoV-2 Delta (3.3%) (Fig 2E). Thirty-three samples failed viral genome sequencing, likely due to low viral load or poor sample preservation. The identification of the SARS-CoV-2 variants using whole-genome sequencing showed one hundred percent concordance with our RT-qPCR assay identifications, highlighting the specificity and accuracy of our assay (Fig 2F). Genetic and phylogenetic analyses of the sequenced genomes show defining mutations of the omicron sublineages and the presence of three distinct clusters corresponding to BA.1, BA.1.1, and BA.2 (Fig 3). The sublineages BA.1 and BA.1.1 were introduced late in 2021 and continued circulating in the Santa Barbara County (SBC) population throughout early 2022. We detected the introduction of BA.2 in the 6th week of 2022, with sustained transmission until the end of our sampling period (Fig 4A, 4C). Our phylogenetic analyses support the local transmission of these variants (Fig 3).

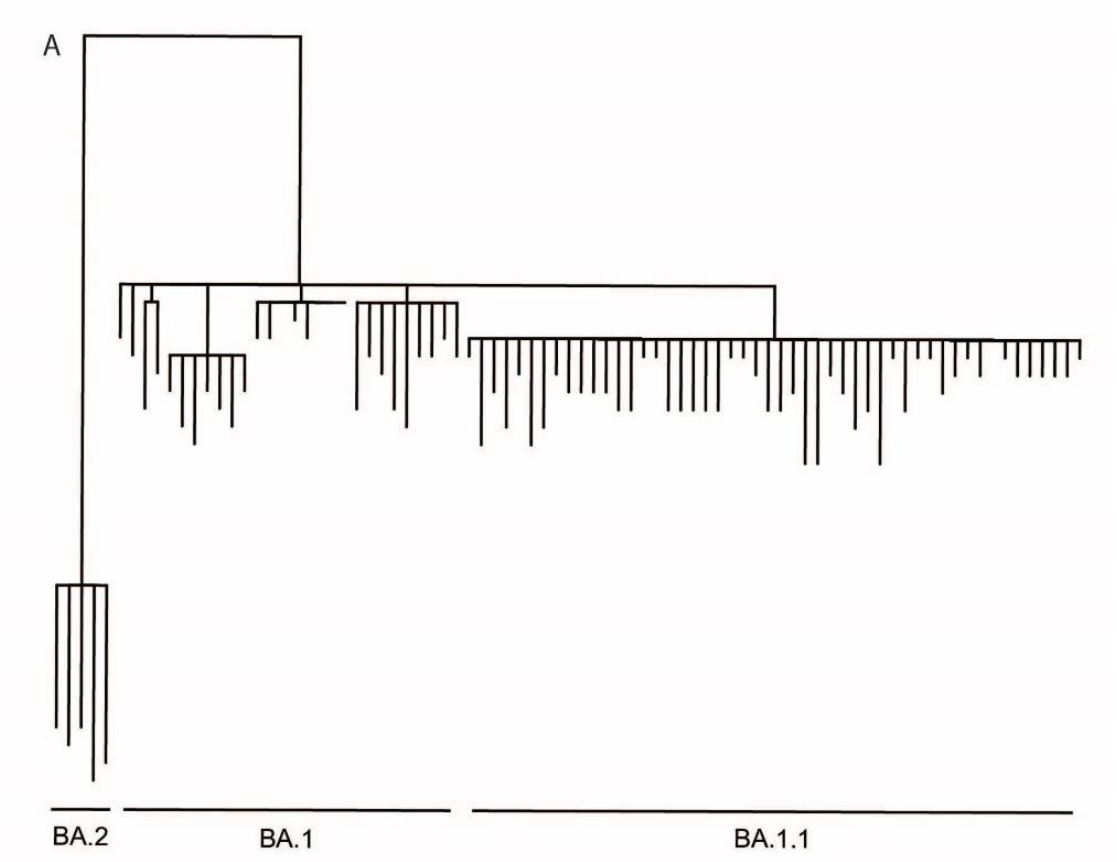

Figure 3. Phylogenetic analysis based on whole-genome sequences of SARS-CoV-2 Omicron variants detected in Santa Barbara County.

The presence of Omicron (BA.1, BA.1.1, and BA.2) in the clinical samples from SBC is linked to a dramatic surge in the number of cases since December of 2021, mainly in the unvaccinated population (Fig 4A, 4B). The weekly distribution of SARS-CoV-2 variants in clinical samples, determined by RT-qPCR (Fig 4C) or whole genome sequencing (Fig 4D), shows the dominance of the Delta variant in SBC throughout November and the initial detection of Omicron in the week of December 5th, 2021. The rapid expansion of the Omicron variant in the population is seen in the following two weeks, with the complete replacement of the Delta variant and the dominance of Omicron found present in 100% of the samples tested by the first

week of January 2022 (Fig 4C). We detected the BA.2 sublineage during the second week of February 2022, with low prevalence (below 5%) throughout the rest of the month.

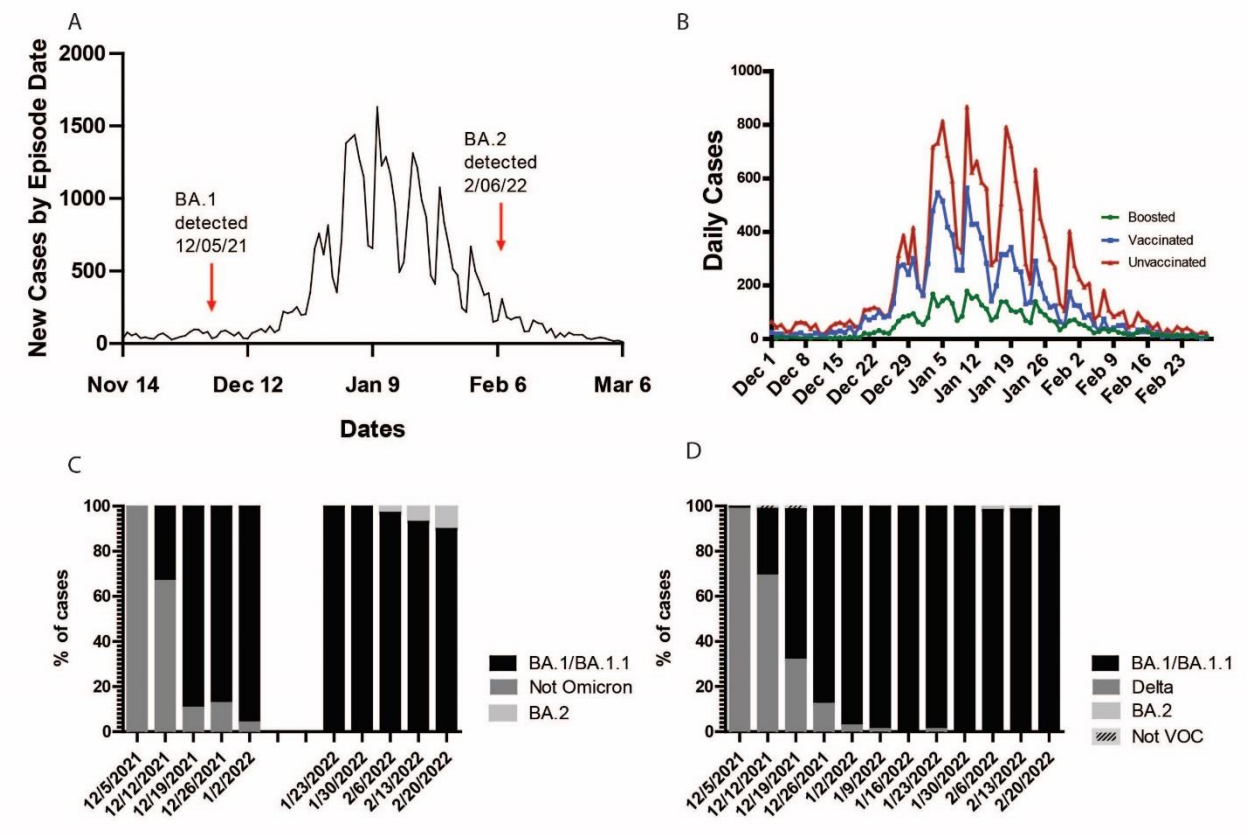

Figure 4. Daily cases and relative variant proportions in Santa Barbara County. (A) Total new COVID-19 cases by episode date and (B) new cases in boosted, vaccinated, and unvaccinated individuals in Santa Barbara County reported by the SBCPHD[117]. (C) Relative proportion of omicron samples in Santa Barbara County, determined via variant-specific RT-qPCR and (D) whole viral NGS.

Discussion

As new SARS-CoV-2 variants emerge and fuel COVID-19 cases worldwide, it is critical to continue developing tools for the rapid identification and characterization of

viral variants that will inform clinical and public health decisions. In SBC, our early adoption of next-generation sequencing methods for genomic surveillance of SARS-CoV-2 became a fundamental part of the local COVID-19 pandemic response. NGS of viral genomes shed light on the regional distribution and prevalence of viral variants and informed prevention and clinical intervention strategies[118]. While informative and critical for early and guided public health responses, state-wide and local next-generation surveillance initiatives provided results with a one to six weeks delay. Omicron's rapid emergence and high transmissibility presented a precipitous local surge risk, as seen in other communities[94]. Thus, the successful control of potential Omicron outbreaks required the prompt detection of this variant in patient samples. From the clinical management perspective, a priori knowledge of the presence and prevalence of Omicron variants in the patient population can help guide the selection and use of limited-supply monoclonal antibody therapies[27].

Many groups around the world have responded to the emergence of these highly infectious variants by developing several assays to detect viral variants of concern[99–107]. In this study, we collaborated with SBC public health officers and clinicians to rapidly develop and implement a simple and highly specific RT-qPCR assay to detect Omicron variants in residual diagnostic clinical samples. The primers we use in this RT-qPCR assay target unique combinations of mutations in the BA.1/BA.1.1 and BA.2 viral genomes, which differentiate this assay from others reported in the literature (see Table 1). With this design, PCR amplification will only occur when the primer binds the cDNA derived from the target viral variants, resulting in the accurate identification of specific viral sublineages. This rapid assay

(4 hours from start to completion) requires basic equipment and reagents commonly found in molecular biology and clinical laboratories, is scalable, and demands minimal optimization.

This simple RT-qPCR-based assay allowed us to rapidly identify the introduction and rapid dominance of Omicron BA.1/BA.1.1 and BA.2 in the SBC community. These valuable data informed clinicians and discouraged the use of monoclonal antibodies to manage active cases. Moreover, identifying Omicron in the SBC population triggered enhanced testing and contact tracing by the SB Department of Public Health to control viral transmission. The success and rapid identification of BA.1/1.1 and BA.2 in patient samples highlight this assay's straightforward design and adaptability. However, the usability of this RT-qPCR-based assay for detecting other emerging viral variants will require careful selection of the amplification regions. The design of primers to achieve specific amplification may be challenging, particularly to differentiate highly similar variants, for example BA.2 and the recently identified BA.4 and BA.5 sublineages[119].

As the COVID-19 pandemic evolves, rapidly deployable variant detection methods will remain indispensable to enhance public health. Our results demonstrate that a simple assay, needing minimal troubleshooting and optimization, successfully captured the introduction of SARS-CoV-2 variants in the population and provided valuable real-time data during emerging surges to guide clinical and public health efforts. Most importantly, this study illustrates the power and impact of collaborative work and open communication between academic research laboratories, clinicians at local hospitals, and public health officers to rapidly respond

to a public health emergency, significantly improving outbreak control responses and public safety.

Chapter 2: Differential Cellular Responses to ZIKV and HSV1 in Human Retinal Organoids Revealed by Single-Cell RNA Sequencing

Abstract

Understanding the retinal impact of viral infections is key in addressing ocular diseases. Here, we investigate how Zika Virus (ZIKV) and Herpes Simplex Virus 1 (HSV1) interact with human retinal organoids (ROs), using single-cell RNA sequencing (scRNA-seq) for detailed analysis. Early-stage ROs exhibit broad susceptibility to ZIKV, with transcriptional profiling indicating robust upregulation of interferon-stimulated genes and the unfolded protein response, suggesting a dynamic cellular defense against ZIKV infection. In contrast, HSV1 infection in mature ROs suppresses innate immune responses and reduces transcriptomic diversity, highlighting distinct viral pathogenesis mechanisms. These differential responses, revealed through scRNA-seq, provide crucial insights into the unique mechanisms of ZIKV and HSV1 in the retina. This study underscores the value of retinal organoids in ocular virology research, significantly enhancing our understanding of viral pathogenesis in sensory organs and potentially informing future therapeutic strategies.

Introduction

Viral infections affecting sensory organs pose a significant public health issue, with the human retina being particularly vulnerable. This specialized tissue, crucial for vision, is at risk from various viruses, notably Zika virus (ZIKV) and Herpes Simplex Virus 1 (HSV1), both linked to severe retinal conditions. ZIKV is associated with congenital abnormalities and has been implicated in retinal defects in infants born to infected mothers[67,120,121]. HSV1, widely prevalent, contributes to a range of ocular diseases, such as herpetic acute retinal necrosis, which can lead to vision impairment or blindness[64].

ZIKV, part of the Flaviviridae family, gained notoriety during the 2015 Brazil outbreak, where it was connected to an increase in microcephaly cases, marked by reduced head size and developmental issues[66]. Recent studies highlight ZIKV's impact on retinal cells, leading to conditions like microphthalmia[69]. Understanding ZIKV's role in causing microcephaly and related eye abnormalities is vital for developing treatments and prevention strategies. In contrast, HSV1, an alpha-herpesvirus, is known for establishing latent infections and causing recurrent issues[71]. It plays a significant role in retinal diseases, especially Herpes Simplex Retinitis (HSR), characterized by retinal inflammation and potentially leading to complications like retinal necrosis[122,123]. Addressing HSV1-induced retinal disease involves understanding the interplay between viral replication, immune responses, and tissue damage, essential for creating effective therapies and prevention methods.

While traditional animal models like rodents provide some insights, they fail to fully capture the complexity and specificity of human retinal pathology due to differences in physiology and immune response[75,76]. This limitation underscores the need for more representative models. For this reason, human retinal organoid systems derived from human pluripotent stem cells (hPSC) are gaining prominence as three-dimensional (3D) culture platforms for studying viral infections and their effects on human retinal development. Retinal organoids, particularly in their early differentiation stages, closely mimic the cell composition and 3D structure of the embryonic human retina, addressing a key shortfall of traditional two-dimensional (2D) culture systems. Once fully differentiated, these organoids represent the cell makeup of a mature human retina, enabling the study of infections that typically take place in human adults[124]. This multifaceted nature of retinal organoids makes them a valuable tool for studying a wide range of retinal pathologies. Despite the advancements in using organoids for viral pathogenesis studies, research specifically focusing on viral infections of retinal organoids at the single cell level is limited. This study aims to fill this gap by utilizing scRNa-seq to study the heterogeneity of infection at the single cell level.

The use of single-cell RNA sequencing (scRNA-seq) in the study of viral infections in retinal organoids (ROs) provides a detailed analysis of cellular heterogeneity and transcriptional responses. This method has significantly improved our understanding of viral pathogenesis, highlighting differences in individual cell responses and delineating host-virus interactions. scRNA-seq's ability to analyze

complex multicellular systems at a detailed level aligns well with the nature of ROs, which are composed of diverse cell types.

In this study, we leverage human retinal organoids and single-cell RNA sequencing (scRNA-seq) to dissect the complex interactions of ZIKV and HSV-1 with retinal cells. This approach allows us to uncover the distinct transcriptional responses elicited by these viruses, revealing how they differentially affect cellular pathways such as the interferon system and unfolded protein response. Particularly, we show that retinal organoids are susceptible to ZIKV infection, affecting various cell types and triggering significant transcriptional changes in Interferon response and unfolded protein response. Our findings also reveal the uniform trajectory of HSV1 infection in mature retinal organoids and its differential impact on cellular responses compared to ZIKV. This research not only enhances our understanding of the pathogenesis of ZIKV and HSV1 in retinal tissues but also underscores the utility of retinal organoids as a comprehensive model for studying ocular viral infections. The insights obtained from this study are crucial for understanding the cellular and molecular dynamics of viral infections in the retina, which could lead to the development of targeted interventions for a variety of retinal diseases caused by these pathogens. This work was done in collaboration with Duncan Proctor.

Results

Early-Stage Retinal Organoids Are Susceptible and Permissive to ZIKV Infection.

To investigate the impact of Zika Virus (ZIKV) infection on the developing retina, we generated retinal organoids (ROs) that emulate the cellular structure and

functionality of the developing retina (Fig. 5A). This approach utilized a modified protocol originally established by Zhong et al [124]. At 60 days post-differentiation, the ROs closely resembled the embryonic retina's developmental stage during the second trimester of pregnancy, containing key cell types relevant to ZIKV-related pathologies (Fig. 5B). We infected these 60-day-old ROs using ZIKV at an estimated multiplicity of infection (MOI) of 1. The susceptibility of ROs to ZIKV was assessed by immunostaining for the viral NS2B protein at 48- and 96-hours post infection (hpi). Notably, NS2B expression was evident at 48-hpi, with an observable radial and internal expansion of infection foci by 96-hpi, indicative of viral replication (Fig. 5C). Furthermore, to ascertain whether ROs can support the generation of infectious virions, we quantified viral titers in supernatants collected at 48- and 96-hpi, observing a time-dependent increase in viral load (Fig. 5D). Collectively, these results validate the suitability of immature ROs as a model for studying ZIKV

infection dynamics

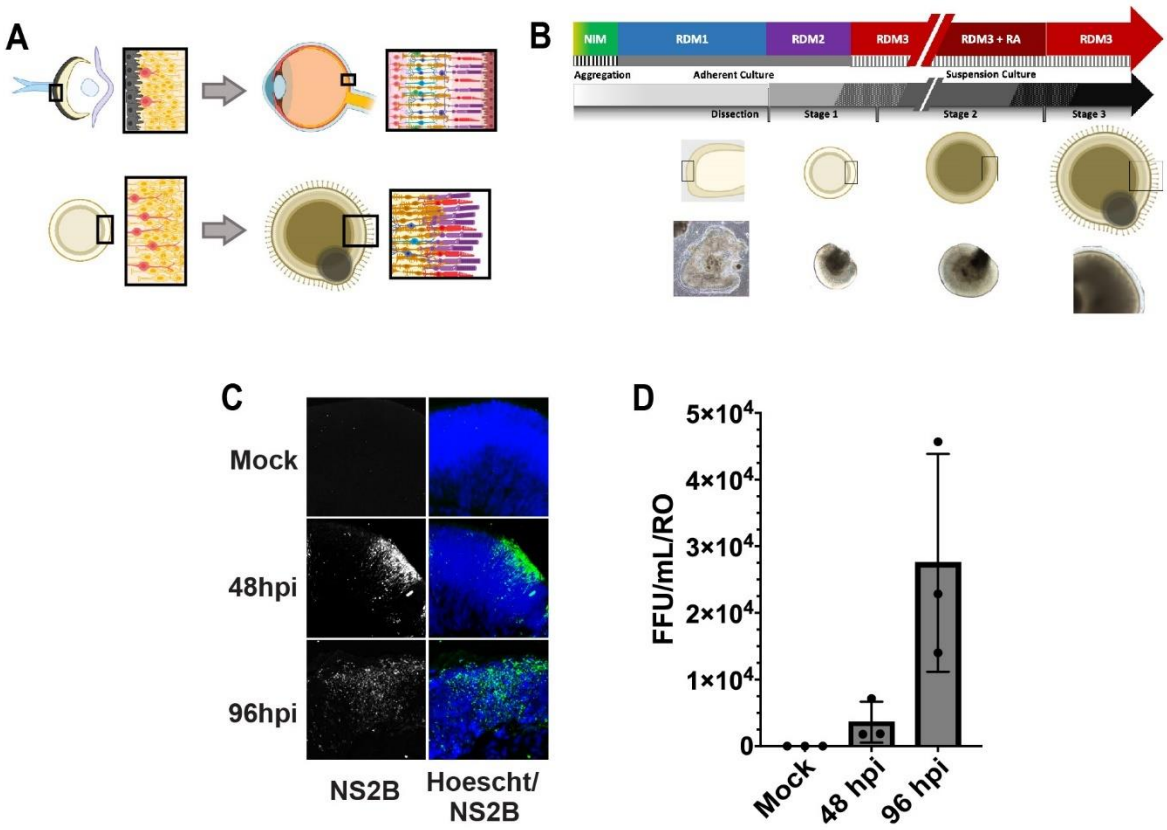

Figure 5. Characterization and ZIKV Infection of Early-Stage ROs. (A) Schematic representation of the protocol used for generating retinal organoids. (B) Schematic representation of the protocol used for generating ROs and brightfield images showing how ROs during the stages of differentiation. (C) Immunostaining of ROs infected with ZIKV, showing the expression of the viral protein NS2B at 48- and 96-hours post-infection (hpi). (D) viral titers measured in supernatants collected from ZIKV-infected ROs at 48- and 96-hpi.

scRNA-seq Analysis Reveals ZIKV Infection Across All Cell Types in Retinal Organoids

To elucidate how ZIKV modifies the transcriptional landscape in retinal organoids (ROs), we employed single-cell RNA sequencing (scRNA-seq). This approach allowed us to capture a comprehensive profile of infection trajectories and cellular responses across different cell types and infection statuses. Although traditional methods require polyadenylated transcripts for capture, the recent establishment of modified protocols for 5' capture allows the capture of ZIKV and other positive sense viruses by utilizing a custom primer spiked into the initial capture reaction (see methods). This methodology enabled us to compare the transcriptomes of uninfected and ZIKV-infected ROs at 24-, 48-, and 96-hours post-infection (hpi), facilitating simultaneous analysis regardless of cell type and infection status. Confirmation of ZIKV infection in the analyzed ROs was achieved by measuring viral titers and assessing cell viability, revealing a predictable increase in viral load alongside a decrease in cell viability in ZIKV-infected ROs (Fig. 6A, B).

We first aimed to determine the extent of ZIKV infection across different cellular populations within immature ROs. To determine cell type within the merged dataset, counts mapped to ZIKV RNA were masked and Leiden clustering was performed. Using gene markers from previous literature, annotation of single-cell identity based on their host transcriptional profile allowed the detection of 8 distinct cellular groups[125–128]. The first 6 groups identified are Müller glia precursor cells (MG), photoreceptor precursor cells (PR), progenitor cells (Prog), retinal ganglion cells (RGC), a mixture of precursor bipolar, amacrine, and horizontal cells

(HC/AC/BP), and cells at an intermediate state of differentiation (Trans). As infection progressed, a group of cells whose transcriptome is defined by high levels of interferon-stimulated gene expression (ISG) grew. Lastly, there was one group of cells with markers matching no known cell type precursor (labeled as Unknown) that has been previously observed in RO scRNA-seq experiments (Fig. 6C). Early ROs are at an intermediate stage of differentiation, containing many precursors to the fully differentiated cell types seen in mature ROs. Notably, the cell groups for horizontal, amacrine and bipolar cells are grouped together due to incomplete differentiation expected in day 60 ROs. The expression of cellular markers for each group are represented in Figure 6E.

Furthermore, our scRNA-seq analysis revealed a broad range of ZIKV RNA counts in infected cells, from zero to over 5000, underscoring the heterogeneity of viral load within the ROs. Across all identified cell groups, we observed a consistent increase in the number of ZIKV-positive cells, from 24-hpi to 96-hpi (Fig. 6D, F). The proportion of ZIKV-infected cells varied across cell types, ranging from 2.9% in photoreceptor cells to 8.2% in Müller glia cells, and as high as 92.5% in the ISG-expressing cell group (Fig. 6G). This data strongly suggests that ZIKV is capable of infecting all cell types present in early-stage ROs.

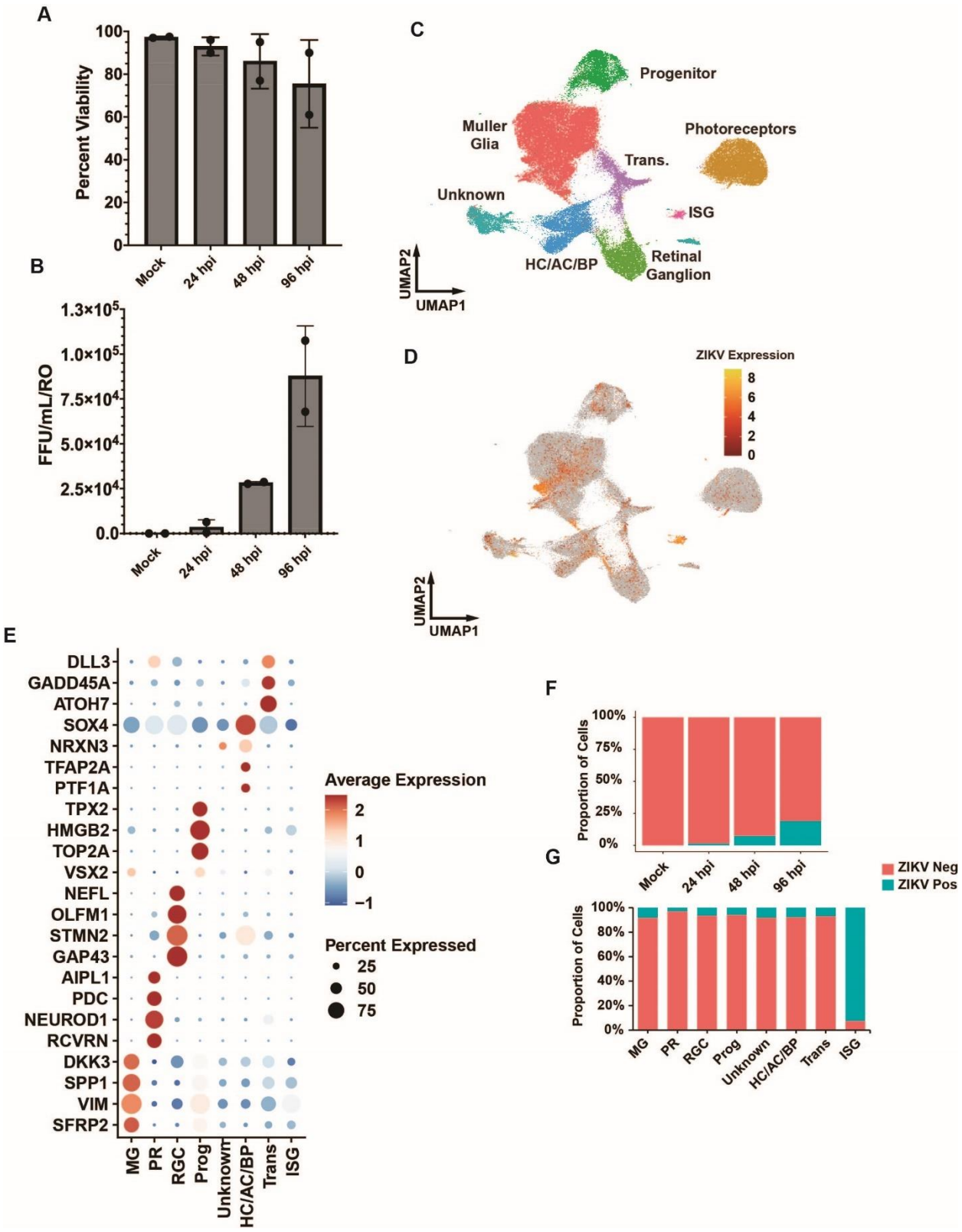
A
Percent Viability
100
80
60
40
20
0
Mock
24 hpi
48 hpi
96 hpi
B
FFU/mL/RO
1.3×10^5
1.0×10^5
7.5×10^4
5.0×10^4
2.5×10^4
0.0
Mock
24 hpi
48 hpi
96 hpi
C
Progenitor
Muller Glia
Photoreceptors
Trans.
Unknown
ISG
HC/AC/BP
Retinal Ganglion
UMAP2
UMAP1
D
ZIKV Expression
8
6
4
2
0
UMAP2
UMAP1
E
DLL3
GADD45A
ATOH7
SOX4
NRXN3
TFAP2A
PTF1A
TPX2
HMGB2
TOP2A
VSX2
NEFL
OLFM1
STMN2
GAP43
AIPL1
PDC
NEUROD1
RCVRN
DKK3
SPP1
VIM
SFRP2
MG
PR
RGC
Prog
Unknown
HC/AC/BP
Trans
ISG
Average Expression
2
1
0
−1
Percent Expressed
25
50
75
F
Proportion of Cells
100%
75%
50%
25%
0%
Mock
24 hpi
48 hpi
96 hpi
G
ZIKV Neg
ZIKV Pos
Proportion of Cells
100%
80%
60%
40%
20%
0%
MG
PR
RGC
Prog
Unknown
HC/AC/BP
Trans
ISG

Figure 6. scRNA-seq Analysis of ZIKV Infection in ROs. (A) Viral titers and (B) cell viability in ZIKV-infected ROs demonstrating an increase in viral load and a corresponding decrease in cell viability between 24- and 96-hpi. (C) UMAP visualization of single-cell RNA sequencing data displaying eight distinct cellular groups identified in immature ROs and (D) corresponding ZIKV expression. The groups include Müller glia precursor cells (MG), photoreceptor precursor cells (PR), progenitor cells (Prog), retinal ganglion cells (RGC), a mixture of precursor bipolar, amacrine, and horizontal cells (HC/AC/BP), cells in an intermediate state of differentiation (Trans), a group defined by high levels of interferon-stimulated gene expression (ISG), and a group with no known cell type markers (Unknown). (E) Selection of cellular markers used to define these clusters. (F) Proportion of ZIKV-infected cells between timepoint and (G) cell group.

Global Transcriptional Response to ZIKV Infection in Retinal Organoids Reveals Interferon Stimulation and UPR Regulation

To explore how the tissue responds to ZIKV infection globally, we analyzed transcriptional responses by infection status. We classified cells into three distinct groups based on their infection status: cells that underwent a mock infection (Mock), cells that were positive for ZIKV transcripts (ZIKV+), and cells that were not positive for ZIKV transcripts but came from organoids that were infected with ZIKV (Bystander). To identify key genes that undergo significant dysregulation upon ZIKV infection, we conducted differential gene expression analysis (DEG) comparing ZIKV+ cells at 48- and 96-hpi to the mock-infected controls. In ZIKV+ cells, many

genes were significantly upregulated (Fig. 7A). Further investigation into broader network activation was performed using Metascape analysis, focusing on genes with over 0.5 log2fold increase and an adjusted p-value below 0.05. The DEG and Metascape analyses revealed a pronounced enrichment of genes associated with the unfolded protein response (UPR) and interferon signaling in ZIKV-infected cells, compared to mock-infected controls (Fig. 7B)[129]. These findings align with existing literature on ZIKV and shed light on the pivotal host responses in ROs during ZIKV infection, potentially influencing the infection's progression.

scRNA-seq has enabled us to determine that all cell types present in early ROs are susceptible to ZIKV infection and to better explore the transcriptional responses of ZIKV infection in ROs. These transcriptional responses play an essential role in determining the outcome of the tissue and provide us with potential targets for inhibiting ZIKV infection in retinal tissue. We next sought to determine whether these transcriptional responses were exclusive to directly infected cells or also present in

bystander cells within the ZIKV-challenged ROs.

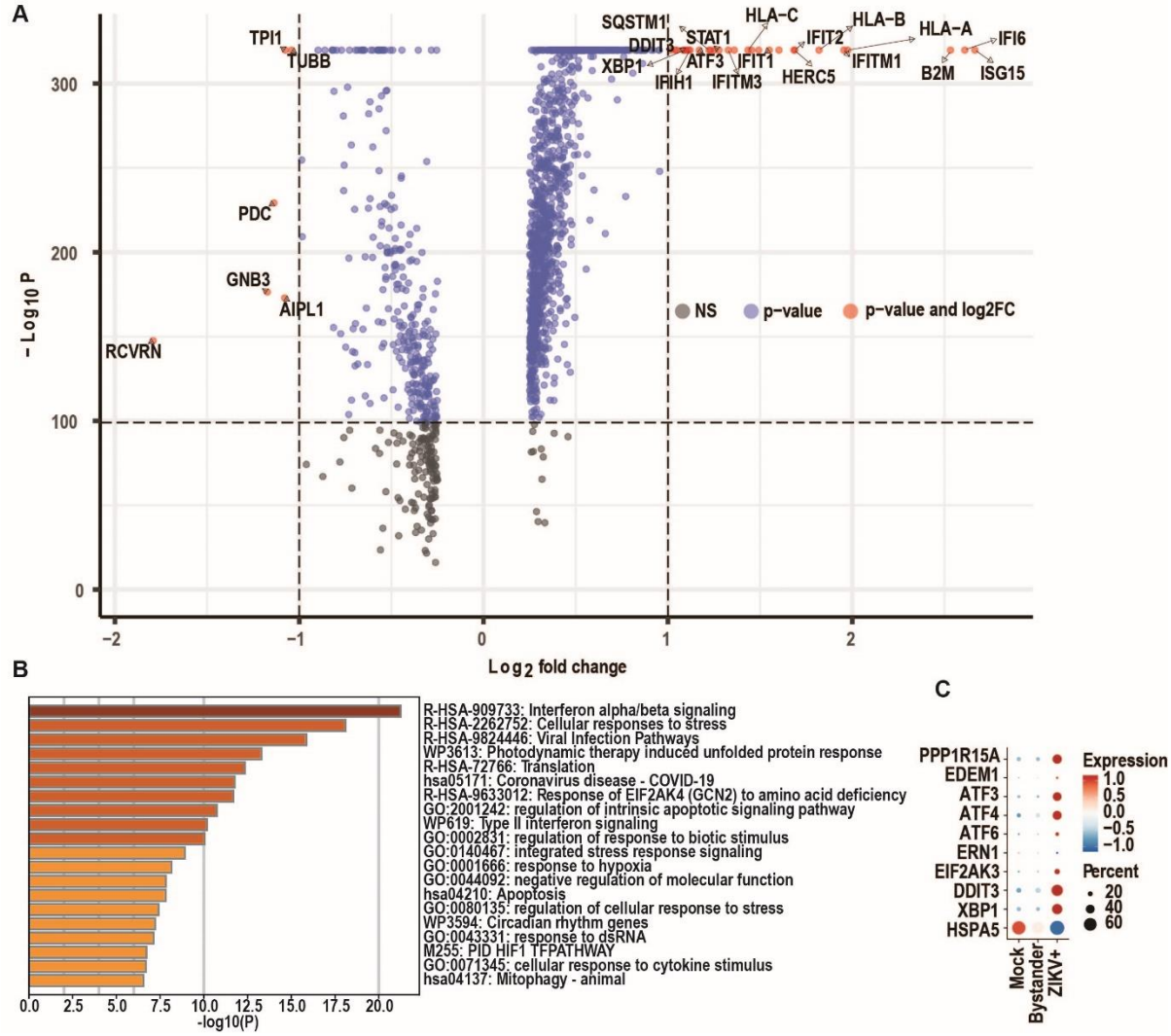

Figure 7. Transcriptional Responses to ZIKV Infected ROs. (A) Volcano plot of the significantly upregulated genes in cells positive for ZIKV transcripts (ZIKV+) compared to mock-infected cells, at 48- and 96-hours post-infection. (B) Metascape analysis on up regulated genes (greater than0.5 log2fold increase and an adjusted p-value below 0.05) reveals a significant enrichment in the UPR and interferon signaling pathways in ZIKV-infected cells. (C)

Expression patterns of genes associated with UPR and ISR in ZIKV-infected ROs.

ZIKV and the UPR

One of the significantly dysregulated gene networks identified from the scRNA-seq in ZIKV infection in ROs were genes involved with the unfolded protein response (UPR) and integrated stress response (ISR). To investigate how those networks are activating, we generated dot plots for genes from the top expressing genes in volcano plots for the UPR and ISR (Fig. 7C) along with other relevant effectors of those pathways to determine how they are activating in ZIKV+ cells against bystander cells when compared to uninfected control ROs. In ZIKV-infected ROs, we observed modest activation of UPR sensors ATF6 and EIF2AK3, alongside a slight downregulation of ERN1. However, stronger upregulation was noted in key UPR effectors such as ATF4, XBP1, and DDIT3, indicating a more significant role of the UPR in the infection's progression. Interestingly, HSPA5, a master regulator of the UPR, was found to be downregulated in ZIKV+ cells, suggesting an overall suppression of the UPR. Specific UPR effectors, including XBP1 and ATF4, and the apoptosis-associated factor CHOP were notably activated in ZIKV+ cells, underscoring the importance of UPR and ISR pathways in the context of successful ZIKV infection.

Activation of Interferon Response in ZIKV-Infected Retinal Organoids

The other significantly dysregulated network in ZIKV infection is the interferon response. We see that during ZIKV infection the relative number of reads increases

in both ZIKV+ and bystander cells when compared to mock infected cells (Fig 8A). This increase is time dependent with the most significant increase in ISG expression observed at 96-hpi. In addition to global ISG expression, individual ISGs are upregulated differentially between ZIKV+ and Bystander cells (Fig 8B).

The increase in ISG expression is generally conserved between ZIKV+ and Bystander cells, with some genes expressed higher in ZIKV+ cells (B2M, HLA-A, HLA-B, …) or bystander cells (IFI6, IFITM3, ISG15, …). Furthermore, we observe that genes like IFI6 are significantly upregulated in cells with little to no ZIKV expression (Fig 8C). An upregulation of the restriction factors IFITM3 and IFITM1 in Bystander cells suggests that the cells are being primed to prevent a viral infection. While the upregulation of MHC class I genes like B2M and the HLA-A/B/C in ZIKV+ cells indicate an increase in ZIKV+ cells capacity to present viral antigens. ISG15, a ubiquitin-like protein that plays a significant role in antiviral defense, is also upregulated in Bystander cells. Interestingly, one of the cofactors required for ISG15's ubiquitin like function, HERC2, is only significantly upregulated in ZIKV+ cells, suggesting a differential antiviral function between Bystander and ZIKV+ cells. All of this supports the idea that Bystander cells have entered an interferon induced antiviral state, while ZIKV+ cells are increasing their potential for activating the adaptive immune system.

We next sought to explore which cells were stimulating this ISG expression. Only 6 interferons were expressed in the dataset, IFNB1, IFNK, IFNL1, IFNL2, IFNL3, and IL6. Surprisingly, only 0.4 percent of the cells (459 cells) in the total dataset express any of the known interferons. Of this 0.4 percent, 64.1 percent of

these cells are present in the ISG cluster. Furthermore, the expression of interferons increased in a time dependent manner with 25 time more cells expressing IFN in the 96-hpi time point than in the mock infected sample. This evidence suggests that the robust ISG response observed in infected ROs originated from a very small number of interferon producing cells.

To investigate the role of type I interferons in modulating ZIKV infection with pre-treated ROs with interferon-alpha and beta to mimic a bystander effect before infection with ZIKV. We determined the effect interferon treatment had on ZIKV replication through tittering. Compared to mock-treated ROs, treatment with either interferon had a near-complete inhibition of titers with a slightly more robust response in IFNa-treated ROs (Fig. 8D). This data supports the immunoprotective effects of type I interferons for limiting ZIKV infection levels identified in bystander cells of infected ROs.

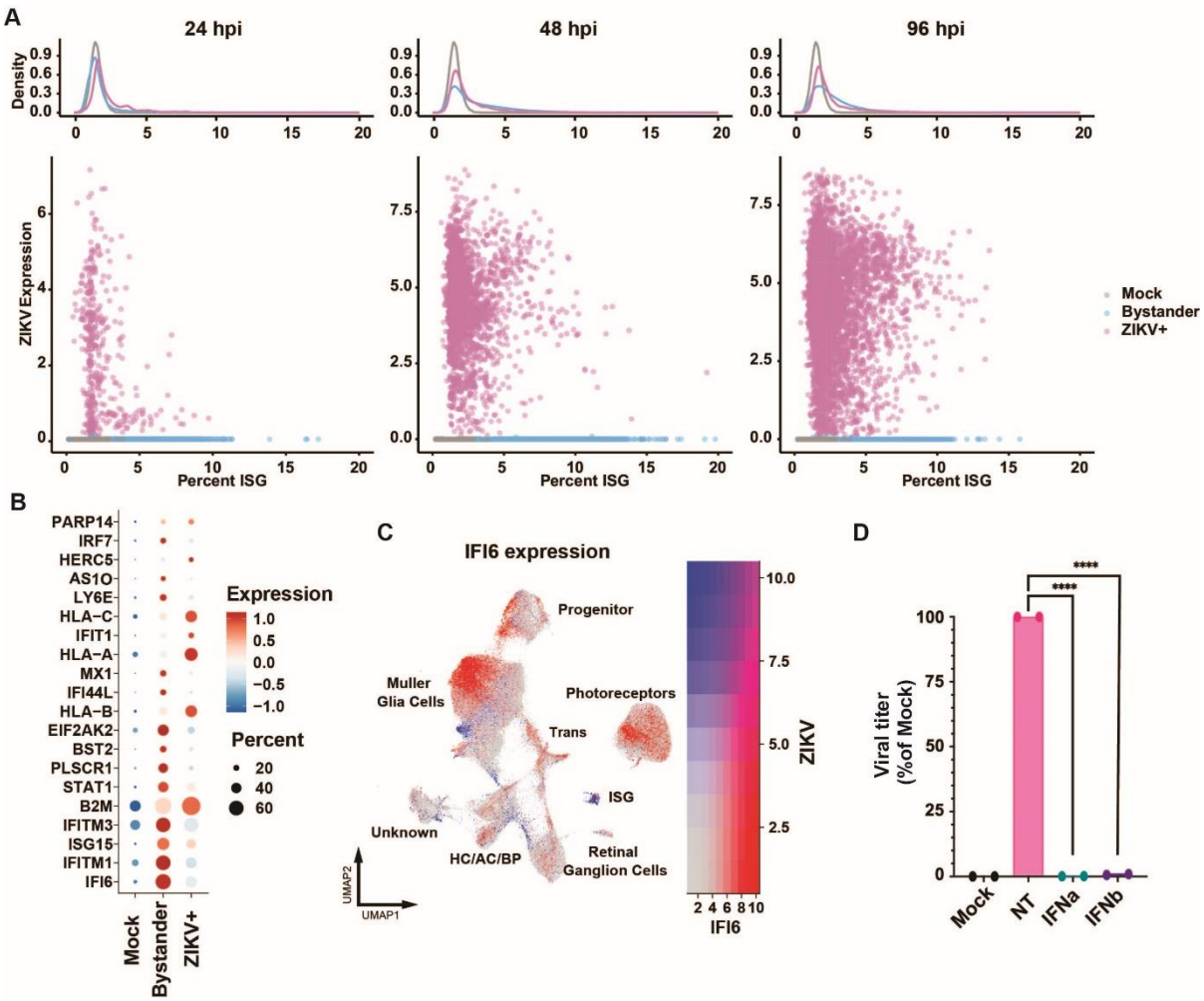

Figure 8. Interferon Response in ZIKV-Infected Retinal Organoids. (A) Scatter plots (bottom) and density plots (top) showing a time-dependent increase in the percentage of reads mapped to interferon-stimulated genes (ISGs) in both ZIKV-infected (ZIKV+) and bystander cells compared to mock-infected cells. (B) Differential upregulation of individual ISGs between ZIKV+ and bystander cells, highlighting the distinct immune response dynamics within infected ROs. (C) Upregulation of IFI6 in cells with minimal or no ZIKV expression, suggesting an enhanced antiviral state in bystander cells. Expression levels arbitrary binned between zero and 10 for visualization. (D)

Pre-treatment with interferon-alpha (IFNa) and beta (IFNb) reduce viral titers in ZIKV infected ROs.

Mature Retinal Organoids Are Susceptible and Permissive to HSV1 Infection.

To explore if the responses observed in ZIKV-infected retinal organoids are conserved across multiple classes of human virus, we measured infection using HSV1 with a GFP-fused US11 protein (HSV1-GFP) in retinal organoids. To better recapitulate ARN and clinically observed retinal phenotypes for HSV1 infection, mature retinal organoids (greater than 180 days post-induction) with mature PRs with outer segments were used for these infections. To determine the initial susceptibility of mature ROs to HSV1, we infected mature ROs with 15,000 pfu HSV1 with a GFP-fused US11 protein (HSV1-GFP) and tracked infection over 48-hpi. From phase imaging in conjunction with the live tagged HSV1-US11-GFP, there is initial plaque establishment at the multiple locations by 8-hpi. Those plaques have rapid internalization to deeper RO structure to near complete infection and the collapse of overall RO architecture by 48-hpi (Fig. 9A). To confirm HSV1 replication in infected ROs, we measured the production of infectious particles over the same infection timeline. As expected, there is a time-dependent increase in viral titers from 8-hpi to 24-hpi, correlating with the rapid replication cycle characteristic of HSV1 in other cell culture models (Fig 9B). The near-complete infection of RO surfaces producing a large amount of HSV1 supports late-stage ROs as a model for mature retinal targeting viruses.

Although we see HSV1 plaque establishment with near complete HSV1 staining by 48-hpi with corresponding titer increases, the identity of the cell types

infected in late ROs remains unknown. Initially, we stained for the type III interfilament protein Vimentin, a cell marker of MGCs, against HSV1-US11-GFP. HSV1 appears to infect MGC due to a strong correlation between regions with vimentin and GFP expression with specific co-staining in Vim+ cells (Fig. 9C). One of the outstanding questions is the susceptibility of ROs to HSV1. When HSV1-US11-GFP is stained against the PR marker Opsin, there is strong HSV1-GFP expression in correlation with opsin, suggesting HSV1 is infecting PRs (Fig 9D). To confirm potential PR infections, we utilized the live GFP tag on HSV1 to image infection progression in mature ROs containing an outer rim of PR outer segments over 24 hours of infection. There was an initial infection in apparent outer segments at 8hpi that expanded through multiple cell layers by 24-hpi (Fig. 9E). Most significantly, our staining of HSV1 infection in late-stage ROs demonstrate that human-derived photoreceptors are susceptible to HSV1, the infection can progress

into internal layers, and targets other major cell types implicated in other studies.

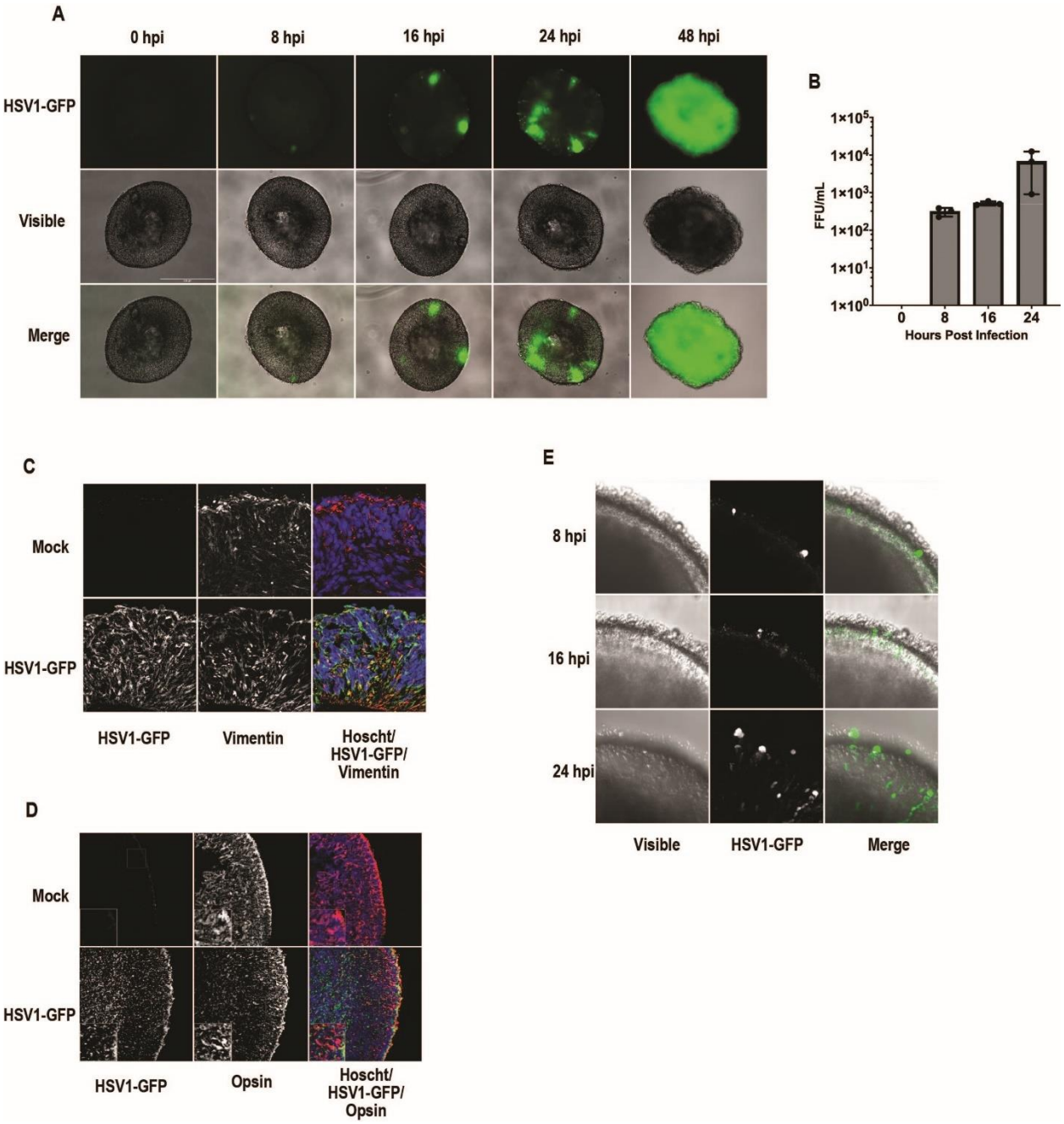

Figure 9. HSV1 Infection Dynamics in Mature Retinal Organoids with GFP-Fused US11 Protein. (A) Phase imaging combined with live tagging of HSV1-US11-GFP shows the establishment of viral plaques within infected ROs. (B) Time-dependent increase in viral titers from 8- to 24-hpi. (C) Co-localization of

HSV1-GFP with Müller glia cell marker Vimentin and (D) photoreceptor marker Opsin, indicating HSV1 infection in these cells. (E) Live imaging using the GFP tag on HSV1 to track infection progression over 24 hours in mature ROs containing an outer rim of PR outer segments. The images show initial infection in the outer segments at 8-hpi, which expands through multiple cell layers by 24-hpi.

Immune Suppression and Transcriptional Alterations in HSV1 Infected Mature Retinal Organoids

To build off our initial findings of HSV1 infection in mature ROs by IHC, we wanted to elucidate the transcriptional landscape of HSV1-infected ROs and compare the nuances or conservation of the transcriptional responses identified from ZIKV infection. To do so, we utilized single-cell RNA sequencing in HSV1 infected ROs at 8-, 16-, 20-, and 24-hours post-infection as well as mock-infected ROs using single-cell RNA-seq. Due to large batch-to-batch variability in mature ROs, we annotated cell types and subtypes within each of the two replicates using Leiden clustering. After filtering for high-quality transcriptomes, cell identity was determined by previously established transcriptional cell type marker lists. 10 unique groups of cells were identified in our HSV1-infected ROs. Initially, we have the expected cell types of late-stage ROs with photoreceptor cells (PR), cone cells (Cones), Müller glia cells (MG), bipolar cells (BP), Progenitor cells (Prog), retinal ganglion cells (RGC) amacrine cells (AC), horizontal cells (HC), cells in an intermediate state of differentiation (Trans) and a group of cells whose transcriptome is defined by HSV1 infection (Fig 10A). Early time points show a low level of infection with a large

increase in the number of infected cells at 24hpi (Fig 10C). This data supports the global infection of major cell types present in mature ROs.

Although we see robust immune modulation by ZIKV, suppression of the innate immune response is a hallmark of HSV1 infection. HSV1 infection leads to a decrease in the overall complexity of the transcriptomic data, as seen in a reduction in the ratio of unique genes detected (UMIs) as well as a loss of cellular identity in infected cells (Fig. 10D, E). The loss of complexity begins early in infection and is likely a consequence of HSV1 induced host shutoff. To explore the role of host shutoff by HSV1 in ROs, we used the highlighted ZIKV-stimulate ISGs as our representative immune genes for HSV1-infected ROs. Gene expression of target ISGs decreases globally in infected and bystander cells (Fig 10F). In both early and late time points, there is a mild decrease in the overall ISG expression observed in both the infected and bystander cell groups compared to mock-infected cells (Fig. 10G). Although ZIKV infection demonstrates the innate immune capability of ROs, the shutdown of those same responses with HSV1 infection highlights a lack of conservation of general antiviral responses and the continued need to expand ROs to model other viral pathologies.

In regards to the UPR, the other major pathway upregulated in ZIKV infection, we observe the opposite effect. Most of the critical genes are upregulated in bystander cells while being largely downregulated in HSV1+ cells. One exception being the upregulation of PPP1R15A (GADD34), suggesting the reversal of translation inhibition via ATF4. This suggests that not only is HSV1 capable of

downregulating the ISG response in infected cells but is also downregulating the UPR in infected cells.

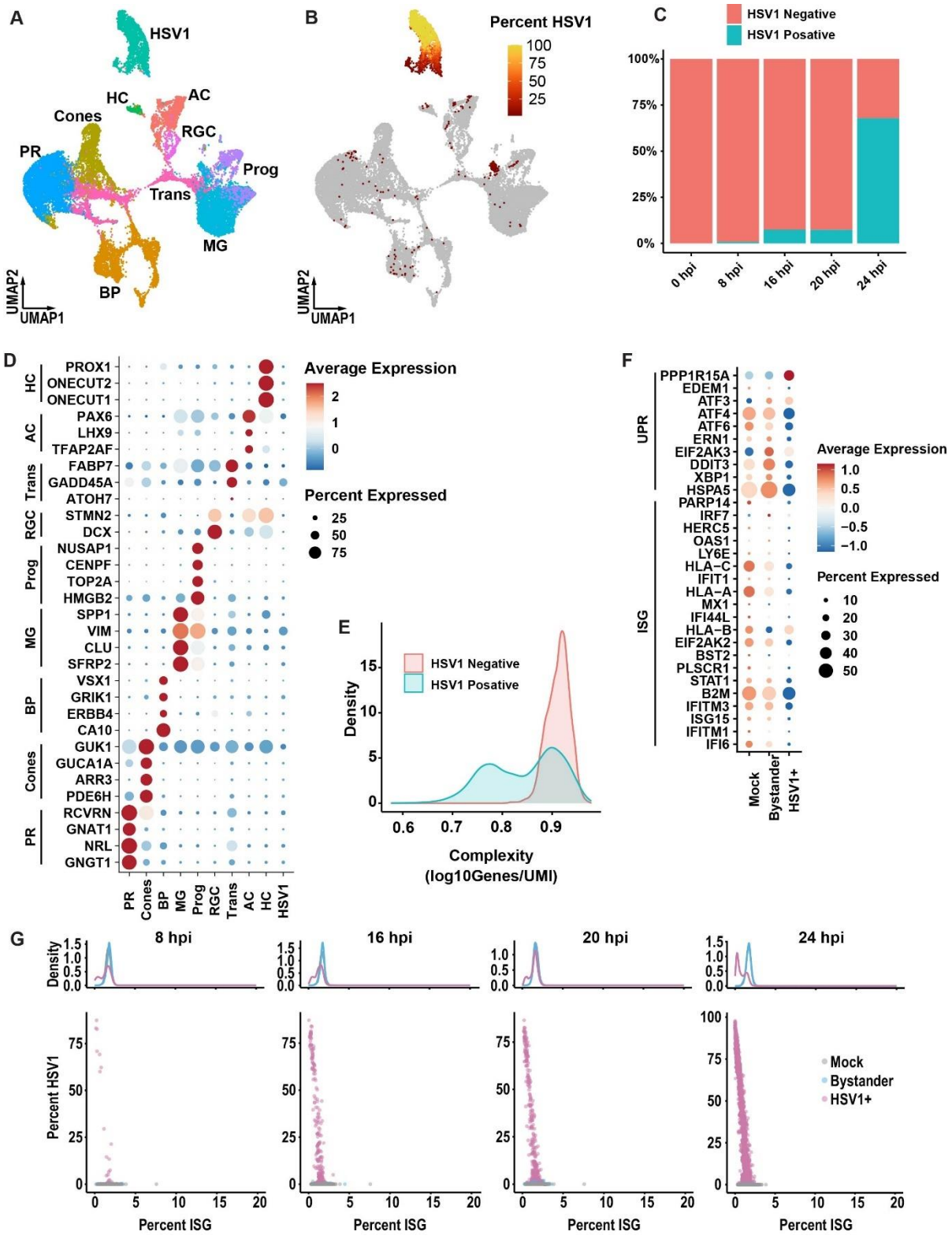

Figure 10. Transcriptional Landscape and Immune Response Alteration in HSV1-Infected Mature Retinal Organoids. (A) UMAP with annotation of cell

groups and (B) infection level in HSV1 infected mature ROs from scRNA-seq data. 10 unique cell groups were identified in HSV1-infected ROs, including photoreceptor cells (PR), cone cells (Cones), Müller glia cells (MG), bipolar cells (BP), progenitor cells (Prog), retinal ganglion cells (RGC), amacrine cells (AC), horizontal cells (HC), cells in an intermediate state of differentiation (Trans), and a group defined by HSV1 infection. (C) Percent of infected cells by timepoint. (D) Representative cell type markers used to define these cell group. (E) Cellular complexity of transcriptomic data between infected and uninfected cells in scRNA-seq data. Complexity is defined as the log10 unique genes divided by the total number of UMI counts for each cell. (F) Expression levels in HSV1 infected ROs for UPR and ISG marked identified in ZIKV infected ROs. (G) Scatter plots (bottom) and density plots (top) showing a time-dependent decrease in the percentage of reads mapped to interferon-stimulated genes (ISGs) in both HSV1-infected cells compared to mock-infected cells.

HSV1 Infection Trajectory in Retinal Organoids.

Lytic HSV1 infection is classified into 4 main categories of viral gene expression: immediate early (IE), early (E), and two late stages (L1, L2). To explore the trajectory of HSV1 infection in ROs, we performed clustering and pseudotime analysis of HSV1 gene expression in infected cells. Trajectory analysis revealed that viral gene expression in infected ROs follows a single trajectory with a linear relationship between percent HSV1 and pseudotime (Fig. 11A, B). Cells whose transcriptome contain a low level of HSV1 transcripts are primarily expressing IE

genes, while cells whose transcriptome contain a high level of HSV1 transcripts are robustly expressing L1/L2 viral genes as is expected (Fig. 11C). This suggests that HSV1 infection progresses in a uniform manner independent of cell type.

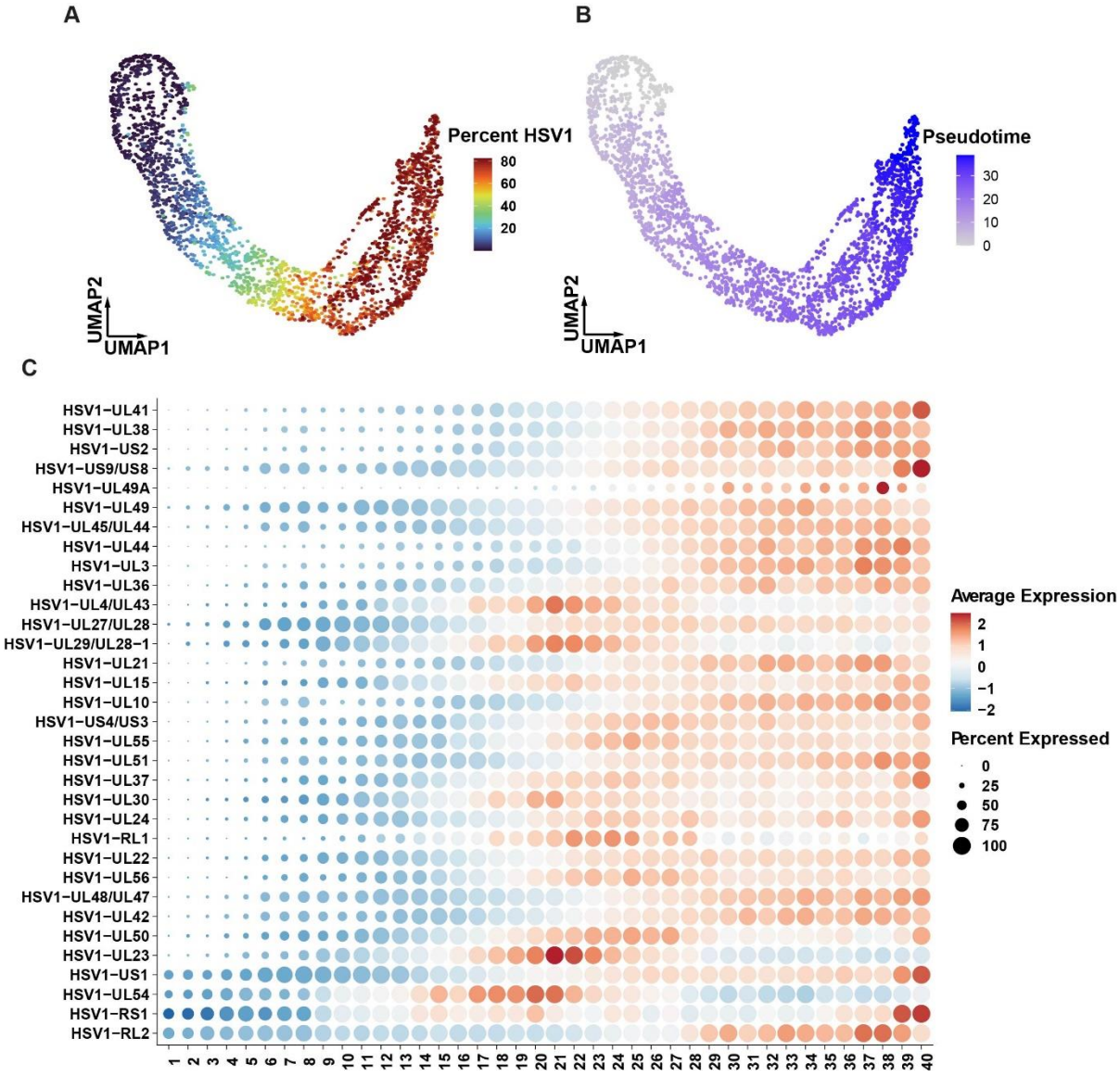

Figure 11. HSV1 Infection Trajectory in Retinal Organoids. (A) UMAP visualization and (B) pseudotime trajectory analysis of HSV1 gene expression in HSV1 positive cells in HSV1 infected ROs. (C) Expression of representative HSV1 genes in HSV1-infected ROs along the pseudotime trajectory.

Discussion

Understanding ZIKV Dynamics in Early-Stage Retinal Organoids

Our study elucidates the susceptibility and permissiveness of early-stage retinal organoids (ROs) to Zika Virus (ZIKV) infection, offering insights into the developmental impacts of ZIKV. The observed increase in viral titers over time, alongside the radial and internal expansion of infection foci, underscores the robust replication capacity of ZIKV in these organoids. These findings are consistent with existing literature highlighting the extensive cellular tropism of ZIKV, particularly in neural tissues. Furthermore, the resemblance of our ROs to the embryonic retina during the second trimester of pregnancy positions them as a crucial model for studying ZIKV's pathogenesis during critical stages of neurodevelopment.

Transcriptional Responses to ZIKV Infection in ROs

The application of single-cell RNA sequencing (scRNA-seq) has provided a detailed landscape of the transcriptional changes within ROs following ZIKV infection. Our observations of a consistent increase in ZIKV-positive cells and the broad range of viral RNA counts highlight the complexity of the infection process. The ability to infect all identified cell groups in the ROs echoes findings from other studies on ZIKV's broad cellular tropism and underlines the virus's potential to cause widespread damage in the developing retina. The heterogeneity in viral load across different cell types may be indicative of varying degrees of cellular susceptibility or antiviral defense mechanisms.

Activation of UPR and ISR in Response to ZIKV

The activation of the unfolded protein response (UPR) and integrated stress response (ISR) in our ZIKV-infected retinal organoids (ROs) highlights a complex interplay of cellular stress mechanisms in response to viral infection. The upregulation of ATF4, XBP1, and DDIT3, key UPR effectors, suggests a robust cellular attempt to mitigate the stress caused by viral protein synthesis and assembly. This observation aligns with existing literature indicating that viral infections can induce ER stress and activate UPR pathways as a cellular coping mechanism. However, the downregulation of HSPA5, a critical regulator of the UPR, might reflect a strategic viral interference, potentially aiming to disrupt the host's stress response to facilitate replication. This finding provides a new perspective on ZIKV's ability to manipulate host cell pathways, adding to the growing body of knowledge about viral-host interactions in the context of retinal infections.

Moreover, the modest activation of UPR sensors like ATF6 and the downregulation of EIF2AK2 and ERN1 indicate a selective activation of the UPR pathway. The regulation of these genes could be an indication of the cell's attempt to balance between managing ER stress and preventing apoptosis. This selective activation of UPR components in response to ZIKV infection has been observed in other viral infections and is thought to play a role in determining cell fate during infection.

In addition to UPR, the limited activation of the ISR, particularly the analysis of EIF2AK3, parallels the observations in UPR sensor activation, suggesting a coordinated response to viral stress. The ISR is a critical pathway in the cellular

response to a variety of stressors, including viral infections. Its activation typically leads to a reduction in general protein synthesis, which can be a defense mechanism against viral replication. The observed limited activation in our study might indicate a partial inhibition or evasion by ZIKV, a strategy that could be employed by the virus to maintain its replicative needs while avoiding complete shutdown of host cellular machinery.

Furthermore, the specific activation of UPR effectors, including XBP1 and ATF4, and the apoptosis-associated factor CHOP in ZIKV+ cells underscores the importance of these pathways in the context of ZIKV infection. The significant role of these effectors in mediating cellular responses to ER stress and their implication in apoptosis aligns with previous research on their roles in viral pathogenesis. In particular, the role of CHOP in promoting apoptosis in response to prolonged ER stress could be an indicator of the cellular outcome following ZIKV infection.

Interferon Response and Its Implications in ZIKV Infection

The interferon (IFN) response activated in ZIKV-infected retinal organoids (ROs) presents a critical aspect of the cellular defense mechanism against viral infections. Our observations of a time-dependent increase in interferon-stimulated gene (ISG) expression in both ZIKV+ and bystander cells highlight the robustness of this response. Notably, genes like B2M, HLA-A, and HLA-B are upregulated more in ZIKV+ cells, indicating an enhanced capacity for antigen presentation. This upregulation suggests an active role of infected cells in signaling to the immune system, potentially facilitating the recognition and elimination of infected cells. The upregulation of MHC class I genes aligns with existing studies, emphasizing their

role in presenting viral antigens to CD8+ T cells, thereby initiating adaptive immune responses (cite relevant studies).

Conversely, the upregulation of genes such as IFI6, IFITM3, and ISG15 in bystander cells points to a state of preparedness against viral infection. IFITM3 is known for its role in restricting viral entry into cells, and its upregulation in bystander cells might reflect a preemptive defensive stance, reducing the likelihood of infection spreading. This pattern of gene expression resonates with the concept of 'antiviral state' often induced by IFN signaling, preparing neighboring cells for potential viral threats.

The role of ISG15, a ubiquitin-like protein, is also noteworthy, especially considering its upregulation in bystander cells. ISG15 is implicated in antiviral defenses, and its modification processes could be critical in shaping the cellular response to ZIKV. Studies have found that knock out of ISG15 leads to worse prognosis in ZIKV infected mice eyes. The differential expression of HERC2, a cofactor for ISG15, between ZIKV+ and bystander cells, suggests that ISG15 may play multiple roles in ZIKV infection. Studies have also shown that overexpression of ISG15 stimulated ZIKV replication, although it did not affect viral entry and was dependent on ISGlyation.

The small percentage of cells expressing known interferons, yet contributing significantly to the robust ISG response, underscores the efficiency of the IFN signaling pathway. This finding supports that a few interferon-producing cells can orchestrate a widespread antiviral response, a characteristic feature of the innate immune response to viral infections. The time-dependent increase in interferon

expression further corroborates the dynamic nature of the immune response in ROs during ZIKV infection.

Furthermore, the differential responses to type I interferon treatment in pre-treated ROs reinforce the protective role of these cytokines against ZIKV infection. The observed near-complete inhibition of viral replication following interferon treatment provides a compelling argument for the potential use of interferons as prophylactic or therapeutic agents against ZIKV.

In summary, the interferon response in ZIKV-infected ROs highlights the intricate interplay between viral infection and the innate immune system. The differential expression of ISGs and MHC class I genes between ZIKV+ and bystander cells provides insights into the cellular strategies employed to combat viral infection and prevent its spread. These observations not only enhance our understanding of the innate immune response to ZIKV but also offer potential targets for therapeutic intervention.

Comparative Analysis with HSV1 Infection in Mature ROs

The susceptibility of mature ROs to Herpes Simplex Virus 1 (HSV1) and the contrasting transcriptional responses compared to ZIKV infection offer valuable insights. Unlike ZIKV, HSV1 infection led to a suppression of the innate immune response, exemplified by the downregulation of ISGs. This stark contrast underscores the specificity of viral strategies in modulating host responses and highlights the importance of using organoid models to study diverse viral pathologies. The differences observed in the UPR between ZIKV and HSV1 further emphasize the unique host-pathogen interactions that define each viral infection.

Conclusions

Our study provides a comprehensive overview of the dynamic interaction between ZIKV and developing retinal tissue, using a novel organoid model. The differential responses observed between ZIKV and HSV1 infections in ROs underscore the complexity of viral interactions with host cells and the importance of context in these interactions. Future studies could build upon these findings by exploring the molecular mechanisms underlying these differential responses and by testing potential antiviral therapies in these organoid models. Moreover, extending this approach to other viruses could further our understanding of viral pathogenesis in neurodevelopmental contexts and aid in the development of targeted interventions for viral infections affecting the retina.

Methods

Cell Lines and Retinal Organoid Differentiation

All cell lines were cultured at 37 °C with 5% CO2 (vol/vol). Vero were cultured in DMEM containing 10% FBS (vol/vol), 2 mM L-glutamine, and 100 U/mL penicillin/streptomycin. Human embryonic H9 line and iPS lines are derived from skin fibroblasts of healthy males and were expanded in mTeSR plus on growth factor reduced Matrigel-coated plates at 37°C and 5% CO2. Retinal organoids were generated using a modified version of the Zhong et al. protocol. Stem cell cultures formed embryoid bodies in Aggrewell plates while transitioning from mTeSR to NIM (by day 2) and were maintained in NIM for the first 20 days. EBs were seeded into 2D culture on day 5 of culture with the addition of 55ng/mL of BMP4 and transitioned

out stepwise by day 20. Cultures are fed retinal differentiation media 1 from day 20 until manual dissection of neural retina domains on day 28. Dissected NR domains self-organize in suspension culture in RDM2 until day 42. ROs are transitioned to RDM3 with FBS to support long-term culture indefinitely. ROs are used at day 60 for our immature experiments and were cultured out to between 180 days and 220 days for the mature organoid experiments.

All cell lines were maintained in an incubator set at 37 °C with 5% CO2 (vol/vol). Vero cells were grown in DMEM supplemented with 10% FBS (vol/vol), 2 mM L-glutamine, and 100 U/mL penicillin/streptomycin. The human embryonic H9 line and iPSC lines, derived from skin fibroblasts of healthy males, were expanded in mTeSR plus media on growth factor-reduced Matrigel-coated plates, also at 37°C and 5% CO2.

For the generation of retinal organoids, we utilized a modified version of the protocol developed by Zhong et al[124]. Stem cell cultures were formed into embryoid bodies (EBs) in Aggrewell plates and transitioned from mTeSR to neural induction medium (NIM; DMEM /F12 1:1, 1% N2 supplement, 1x NEAA, 2ug/mL Heparin) by day 2. These EBs were maintained in NIM for the initial 20 days. On the fifth day of culture, EBs were seeded into a 2D culture system with the addition of 55ng/mL of BMP4 and were gradually transitioned out of this system by day 20. From day 20 onwards, the cultures were fed with retinal differentiation media 1 (RDM1; DMEM /F12 3:1, 2% B27 supplement without Vit. A, 1x NEAA), continuing until manual dissection of neural retina (NR) domains on day 28. Post-dissection, NR domains were cultured in suspension in RDM2 (DMEM/F12 3:1, 2% B27 with

Vitamin A, 1x NEAA) until day 42, allowing for self-organization into retinal organoids (ROs). For long-term culture, ROs were transitioned to RDM3 (DMEM/F12 3:1, 2% B27 with Vitamin A, 1x NEAA, 10% FBS and 100 µM taurine), supplemented with FBS. We utilized ROs at day 60 for experiments involving immature organoids. For mature organoid experiments, ROs were cultured for extended periods, ranging from 180 to 220 days.

Virus Propagation and Tittering

The ZIKV strain PRVBC59, isolated from Puerto Rico in 2015, was cultivated in Vero cells. Infection was initiated at a multiplicity of infection (MOI) of 0.01, and the virus was harvested 96 hours post-infection, with 100 mM HEPES added to the medium. To clarify the virus-containing supernatants, they were centrifuged at 350Xg for 5 minutes and then passed through 45µm PVDF membrane syringe filters (Genesee). The viral particles were subsequently concentrated approximately 3-fold using Amicon Ultra-15 Centrifugal Filters (Millipore), with centrifugation set at 1.5xg for 10 minutes. The virus was aliquoted and stored at -80°C. The viral titers of frozen aliquots were quantified through focus assays conducted on Vero cells infected for 30 hours and using mouse anti-envelope staining to detect viral foci.

The Herpes Simplex Virus 1 (HSV1) US11-GFP variant was propagated in Vero cells at an MOI of 0.01 and harvested at 48 hours post-infection. To lyse the cells and release the virus, the infected cell cultures underwent three freeze-thaw cycles, consisting of flash freezing at -80°C for 5 minutes and thawing at room temperature. The mixture of lysed cells and supernatant was centrifuged at 300xg for 10 minutes, followed by filtration using a 45µm PVDF membrane filter. The virus was aliquoted

and stored at -80°C. For titer determination, the aliquots were thawed and used to infect Vero cells. The presence and quantity of the virus were assessed by counting GFP-positive plaques, indicating active HSV1 infection.

Pharmacological Inhibition and Interferon Treatments

For all treatments, compounds were initially prepared as 1000X concentrated stocks in their respective vehicles to minimize DMSO toxicity. These stocks were further diluted to a 1:1000 working concentration in Retinal Differentiation Medium 3 (RDM3) for application to the retinal organoids (ROs). Prior to infection, ROs were pre-treated with these diluted compounds for 24 hours under standard cell culture conditions. For ZIKV infection, the organoids were immersed in ZIKV stocks diluted in RDM3 to achieve a multiplicity of infection (MOI) of 1, and this exposure was maintained for 2 hours. Correspondingly, mock infections involved a similar ratio of DMEM-to-RDM3 but without the virus. Following the infection period, the virus-containing medium was discarded, and the organoids were then bathed in fresh RDM3 supplemented with the respective treatment compounds. Supernatants were collected at designated hours post-infection for analysis and were immediately replaced with fresh RDM3 containing the ongoing treatments.

Tissue Sectioning

Formaldehyde fixed ROs were processed for paraffin or cryo-embedding and sectioning. For cryosectioning, ROs were initially cryoprotected via sucrose penetration with a final transition to OCT; 15% sucrose, 30% sucrose, and then OCT, all at room temperature (RT) overnight or until sinking. Then, ROs were frozen

in molds with 100% OCT on a metal block submerged in dry ice and above liquid nitrogen vapor for 30-60 seconds. Long-term storage of blocks was at -20ºC. Sections were cut at a 5º angle and 16ºC on the Leica CryoStat at 14-20 um onto positively charged slides, bound to slides for 48-96 hours at room temperature, and returned to -20ºC for storage.

RO Immunohistochemistry

FFPE sections underwent deparaffinization via the reverse order of paraffinization. Heat-induced antigen retrieval was performed for all formalin-fixed, paraffin-embedded tissues and some formalin-fixed cryo-sectioned organoids using 10mM sodium citrate buffer or Tris-EDTA buffer for 20 min. Slices were incubated in blocking buffer containing 3% BSA (vol/vol) and 0.1% Triton X-100 in PBS pH 7.4 for 1 hour at room temperature. Primary antibodies were diluted in 3% BSA (vol/vol) in PBS overnight at 4ºC. After 3x PBS washes, secondary antibodies were diluted in PBS and applied to sections for 1 hour at RT. After 3x PBS washes, slices had a final ddH2O wash before mounting with ProlongGold Antifade reagent and sealed with nail polish. Images were collected with a Leica TCS SP8 confocal microscope. Stained slides were stored at 4ºC, protected from light. Secondary controls were treated with 3% BSA without antibodies instead of primaries.

scRNA-Seq Library Preparation

For each experimental condition, four to five organoids were infected, using an MOI of 1 for ZIKV in immature ROs and 15,000 pfu per RO for HSV1 in mature ROs. The organoids underwent an initial wash with DPBS and were then subjected to

enzymatic digestion using the papain digestion kit (Worthington) with DNase supplementation for 60 to 90 minutes at 37°C. To enhance digestion, mechanical trituration was performed using P1000 and P200 pipettes every 15 minutes until a single cell suspension was obtained. The cell suspensions were centrifuged at 300xg for 5 minutes and washed twice with DPBS. Cells were resuspended in approximately 100 µl of DPBS containing 0.04% BSA (w/v), filtered through a 40 µm cell strainer (Flowmi), counted using a Countess 2 (ThermoFisher), and maintained on ice until further processing.

For scRNA-seq library generation, samples were captured on the 10x Genomics Chromium instrument, allocating one lane per sample, with four samples per run. ZIKV-infected ROs utilized the 5’ reagent kit, while HSV1-infected ROs used the 3’ reagent kit, adhering to the manufacturer's guidelines. The scRNA-seq libraries for ZIKV-infected ROs were prepared using the 10x Genomics Chromium 5’ Gene Expression Kit, with a modification to include two ZIKV-specific primers for capturing and amplifying ZIKV transcripts. Cell mixtures were loaded onto chromium chips, targeting a capture of 2,500 to 7,500 cells per sample. Library preparation followed the manufacturer’s instructions and sequencing was performed on an Illumina NovaSeq, aiming for 50,000 reads per cell. The resulting BCL files were processed using the 10x Genomics Cell Ranger pipeline.

scRNA-Seq Data Analysis

CellRanger software was utilized to process the raw sequencing data[130]. A custom reference genome combining the human genome (GRCh38) and the viral genome was created using CellRanger’s “mkref” function. For the ZIKV dataset, the

reference included the entire ZIKV genome (KU501215.1), while for HSV1, the reference was designed to include mappings to all exons in the X14112.1 genome, with some genes amalgamated to address overlapping 3' transcript regions. Sequencing reads were aligned to these specific reference genomes, and UMI counts for each host gene and viral RNA in each cell were quantified.

The resulting cell by gene matrix for each sample underwent processing with DoubletFinder for the identification and removal of doublets[131]. In the ZIKV dataset, filters for cell quality included a minimum of 300 genes and 500 UMI counts, with a mitochondrial content threshold set at 30%. In contrast, the HSV1 dataset employed a minimum requirement of 50 genes, a lower threshold justified by the dominant expression of HSV1 genes in the dataset. Setting higher thresholds in this case would risk excluding cells with high viral loads.

Data analysis was executed using the Seurat package within R[132]. For the ZIKV datasets, normalization and integration of samples were performed utilizing standard Seurat protocols. Principal Component Analysis (PCA) was conducted, and Uniform Manifold Approximation and Projection (UMAP) was generated using the first 50 principal components. Cell clustering was carried out at a resolution of 1.6, with cluster markers identified through the MAST function in Seurat's "FindAllMarkers". Clusters were further refined to remove low-quality cells and annotated based on well-established cell type markers for ROs[125–128]. Differential gene expression analysis between cell groups was performed using MAST, with Metascape analysis applied to genes exhibiting at least a 0.5 Log2fold increase in expression and a p-value less than 0.05[129]. Figures were produced

using Seurat's built-in functions and ggplot2, with volcano plots visualized via the EnhancedVolcano package in R[133].

For the HSV1 dataset, due to significant batch-to-batch variability in mature organoids, cell groups were clustered and labeled individually prior to dataset integration. This approach was essential to retain cellular resolution that might have been compromised by integrating datasets before cell type identification. Pseudotime analysis of cells infected with HSV1 was conducted using the Monocle2 package[134].

Chapter 4: Conclusions and Future Directions

Preventing pandemics through robust screening.

The onset of a pandemic often begins with the unnoticed spread of a new pathogen, making early detection key in preventing its escalation. Historical experiences, such as the COVID-19 pandemic and the H1N1 influenza outbreak, have underscored the necessity for rapid identification of infectious agents. Robust screening is pivotal in pandemic management, enabling early detection of pathogens crucial for timely containment and mitigation strategies. By identifying infectious agents early, health systems can implement targeted interventions, reducing public health impacts and averting full-scale pandemics.

Current pandemic screening methods, while advanced, face distinct challenges, especially in low-resource settings. These challenges involve balancing ease of development with practical application. On one hand, assays like qPCR and NGS can be developed quickly for high throughput testing, but their feasibility is often

limited in resource-constrained areas. On the other hand, more deployable options such as Lateral flow assays or colorimetric-based assays are better suited for developing countries but require more resources for development and typically have lower throughput. Furthermore, assays intended for lower-resource regions need to be user-friendly, durable, and stable under varying environmental conditions, adding complexity to their development and logistics.

Considering these constraints, I propose a stepwise approach to developing assays for global outbreak monitoring. Firstly, there should be continuous global monitoring of all emerging pathogens at the genomic level, including targeted sequencing of known pathogen variants and de novo sequencing for detection of unknown pathogens. Newly identified pathogens should be studied further, focusing on their pathogenicity and mutation potential. Initiatives like the WHO's Global Outbreak Alert and Response Network and the GISAID platform are currently facilitating this worldwide monitoring and data sharing but will likely require additional resources.

Secondly, the genomic data gathered should be used to develop assays capable of detecting nucleic acids from all known pathogens. AI and machine learning algorithms could expedite this process by designing the framework of the assay, including determining the most appropriate assay type (qPCR, LAMP, NGS, etc.) and creating theoretical components like primers and reaction conditions.

Thirdly, pathogens should be ranked and monitored based on their global health risk. Dedicated research teams should optimize the initial assay parameters in the lab and develop robust diagnostic assays deployable worldwide on short notice.

Often, the development of these assays requires high complexity labs, such as BSL3 or BSL4 facilities, which are scarce in developing countries. High-resource assays like lateral flow or colorimetric detection assays, requiring significant development, should be prioritized based on global health risks.

Lastly, the global community must be constantly utilizing these tools in an effective manner to monitor global pathogens. This includes constantly utilizing population-based approaches like community wastewater testing as well as being prepared to rapidly deploy the more complex diagnostic tools during emerging outbreaks. Although resource-intensive, the COVID-19 pandemic has taught us that rapid response is crucial in preventing global outbreaks. The cost of deploying these diagnostics pales in comparison to the financial and human costs of allowing another outbreak to escalate to a pandemic.

In summary, a proactive, globally coordinated effort in developing and deploying diagnostic assays is essential for effective pandemic preparedness and response. This approach balances technological advancement with practical deployment considerations, ensuring readiness for future global health challenges.

Spatial sequencing of infected ROs

Much of the work presented in this thesis focuses on using single-cell RNA sequencing (scRNA-seq) to determine infection levels and transcriptional responses in the context of ZIKV in retinal organoids (ROs). A notable limitation of traditional scRNA-seq is the loss of spatial information, as cells are dissociated before being barcoded. Consequently, it becomes challenging to ascertain how transcriptional responses are related among neighboring cells. For example, it's unclear whether

cells classified as bystanders are in direct proximity to infected cells or isolated from infection zones. Moreover, transcriptional responses specific to bystander cells might be diluted by including cells far from the infection site, potentially naive to the infection, thereby diminishing the observed aggregate transcriptional response.

To address this limitation, I propose employing spatial sequencing techniques for studying ZIKV in ROs. Advanced tools like 10X Genomics Visium sequencing, which allow for transcriptional analysis from a sectioned slice of cells, offer a solution. This method would enable the determination of transcriptional responses specific to cells in direct proximity to ZIKV infection. It's conceivable that the responses observed in aggregated data are more pronounced in these cells than in those located further from infection foci. This approach might also uncover transcriptional responses unique to cells near infected cells, providing a clearer illustration of their roles. For instance, the limited cells expressing interferons may be situated close to infected RO areas, explaining the low number of interferon-expressing cells. Furthermore, the complex unfolded protein response (UPR) transcriptional profile observed in aggregate data might be a result of distinct UPR profiles - one from cells near the infection and another from cells further away.

Spatial sequencing could also enhance understanding of how these responses are stimulated. If responses are more intense near infected cells, this might indicate primary autocrine signaling, whereas responses observed further from infection foci could suggest paracrine signaling that travels through the media to distant locations.

Additionally, this technique could provide better resolution in determining the susceptibility of different cell types to ZIKV infection. Cell types like photoreceptors

might be less susceptible to ZIKV infection than others but could still be infected similarly due to their proximity to the exterior of the RO. Thus, spatial sequencing offers a more nuanced understanding of infection patterns and cellular responses within the complex microenvironment of ROs, potentially leading to novel insights into ZIKV pathogenesis and host-virus interactions.

In conclusion, employing spatial sequencing in studying ZIKV-infected ROs promises a deeper understanding of viral infection dynamics at a cellular level, offering valuable insights into ZIKV pathogenesis. This approach is poised to significantly advance virology and cellular biology research, paving the way for more targeted and effective strategies against viral infections.

Investigating ZIKV Infection in the Retina through Microglia Co-cultured Organoids

Microglia, as the central nervous system's primary immune cells, play a crucial role in responding to viral infections, particularly in the retina[135]. This is especially relevant in the context of Zika Virus (ZIKV), known for causing neuroinflammation and retinal damage. Currently, a significant limitation of retinal organoids (ROs) is their lack of microglia, which hinders a comprehensive understanding of the retinal immune response to ZIKV[135]. To address this gap, integrating microglia into existing RO models, followed by ZIKV infection, is proposed[136]. This approach, which has been informative in brain organoid studies of viral infections, offers a more accurate simulation of the retinal microenvironment, allowing for the study of dynamic interactions between ZIKV, retinal cells, and microglia[137].

This innovative method will enable the real-time observation of interactions between microglia and ZIKV-infected retinal cells, providing insights into how microglial activation correlates with the level of ZIKV infection. Such observations are key to understanding the overall retinal response to ZIKV infection, including whether microglia contribute to exacerbating or mitigating retinal damage. The co-culture approach is poised to reveal unique transcriptional responses of microglia to ZIKV infection, shedding light on their roles in neuroinflammatory responses, potentially influencing the severity of ZIKV-induced retinal damage.

Furthermore, this method allows for the investigation of neuroprotective functions of microglia against ZIKV infection, such as debris clearance and secretion of protective factors. Additionally, it could provide insights into whether microglia can modulate the spread of ZIKV within the retinal tissue, either containing or inadvertently facilitating the virus's dissemination. Identifying the specific factors or conditions that trigger microglial activation in response to ZIKV will enhance our understanding of their role in viral pathogenesis.

Importantly, this research could lead to the development of therapeutic strategies targeting microglial pathways, offering new treatments for ZIKV-induced retinal damage. Incorporating microglia into ZIKV-infected ROs promises to offer a comprehensive view of the interplay between viral infection, retinal cells, and innate immunity, potentially leading to novel insights into ZIKV pathogenesis and therapeutic approaches.

HSV1 and retinal infections

While our studies have successfully elucidated the dynamics of Herpes Simplex Virus 1 (HSV1) infection in mature retinal organoids, a critical gap remains in understanding the factors that contribute to the autoimmune damage observed in the human retina during HSV1 infection. Notably, despite the robust inhibition of the innate immune response by HSV1, clinical observations indicate significant autoimmune damage in the retina. This paradoxical scenario raises the question of what factors drive this autoimmune response, despite the virus's ability to suppress innate immunity.

The application of coculture models with microglia cells, mentioned above, could provide insights into this question. Additionally, the coculturing of infected ROs with other immune cells, such as T cells and macrophages, and check for IFN secretion and macrophage infiltration may provide insight into viral induced immune damage. This approach is particularly relevant given the upregulation of MHC class I molecules in ZIKV-infected ROs, which could imply a significant role for T cell activation in the autoimmune response.

Another consideration is the potential for molecular mimicry to contribute to the autoimmune response. This phenomenon, where viral antigens resemble host proteins, triggering an immune response against the body's own tissues, could be a key factor in the observed retinal damage and would explain the discordance between sequencing data and clinical observations.

Moreover, the detection of pro-inflammatory cytokines warrants attention. It's possible that the immune responses in HSV1-infected ROs manifest predominantly

at the protein level, with cytokines like IL-1 and IL-6 being released without significant changes in their gene expression patterns. This hypothesis suggests that the window for cytokine release in HSV1-infected ROs might be brief and challenging to capture using scRNA-seq.

Finally, examining HSV1 in recently post-mortem retinas could offer a more comprehensive understanding of the virus's impact on the immune response. Such studies could clarify whether the immune suppression observed in ROs also occurs in more physiologically relevant settings, providing a more holistic view of HSV1's interaction with the human retina.

Testing of HSV1 infected early ROs and Testing of ZIKV infected Mature ROs

In our investigation of Zika virus (ZIKV) and Herpes Simplex Virus 1 (HSV1) in retinal organoids (ROs), we strategically selected the developmental stages of ROs that align with the clinical manifestations of these infections. For ZIKV, we focused on immature retinal organoids to explore congenital retinal deformations resulting from in utero ZIKV exposure. Conversely, for HSV1, we used mature retinal organoids that more closely mimic the structure of an adult retina, including fully differentiated photoreceptor cells.

While the findings from these experiments offer clinically relevant insights, comparing the effects of ZIKV and HSV1 is challenging due to the different stages of organoid development used in our study. Therefore, a critical next step in our research is to assess the impact of ZIKV on mature retinal organoids and HSV1 on immature ones. This approach will enable us to determine whether the unique

immune responses observed in ZIKV-infected organoids are a result of their developmental stage rather than a virus-specific response. Such a study could reveal more about virus-specific mechanisms by contrasting the effects of ZIKV and HSV1 on organoids at equivalent stages of differentiation.

Furthermore, investigating HSV1 in immature organoids could enhance our understanding of congenital HSV1 infections of the retina, a condition also observed in newborns. This research could provide valuable insights into the pathophysiology of these viral infections and inform the development of targeted therapies and preventative strategies.

References

1. Heather, J.M.; Chain, B. The Sequence of Sequencers: The History of Sequencing DNA. *Genomics* **2016**, *107*, 1–8, doi:10.1016/j.ygeno.2015.11.003.
2. McCombie, W.R.; McPherson, J.D.; Mardis, E.R. Next-Generation Sequencing Technologies. *Cold Spring Harb Perspect Med* **2019**, *9*, a036798, doi:10.1101/cshperspect.a036798.
3. Capobianchi, M.R.; Giombini, E.; Rozera, G. Next-Generation Sequencing Technology in Clinical Virology. *Clinical Microbiology and Infection* **2013**, *19*, 15–22, doi:10.1111/1469-0691.12056.
4. Houldcroft, C.J.; Beale, M.A.; Breuer, J. Clinical and Biological Insights from Viral Genome Sequencing. *Nat Rev Microbiol* **2017**, *15*, 183–192, doi:10.1038/nrmicro.2016.182.
5. John, G.; Sahajpal, N.S.; Mondal, A.K.; Ananth, S.; Williams, C.; Chaubey, A.; Rojiani, A.M.; Kolhe, R. Next-Generation Sequencing (NGS) in COVID-19: A Tool for SARS-CoV-2 Diagnosis, Monitoring New Strains and Phylodynamic Modeling in Molecular Epidemiology. *Current Issues in Molecular Biology* **2021**, *43*, 845–867, doi:10.3390/cimb43020061.
6. Pervez, M.T.; Hasnain, M.J. ul; Abbas, S.H.; Moustafa, M.F.; Aslam, N.; Shah, S.S.M. A Comprehensive Review of Performance of Next-Generation Sequencing Platforms. *Biomed Res Int* **2022**, *2022*, 3457806, doi:10.1155/2022/3457806.
7. Ardui, S.; Ameur, A.; Vermeesch, J.R.; Hestand, M.S. Single Molecule Real-Time (SMRT) Sequencing Comes of Age: Applications and Utilities for Medical Diagnostics. *Nucleic Acids Res* **2018**, *46*, 2159–2168, doi:10.1093/nar/gky066.
8. Rhoads, A.; Au, K.F. PacBio Sequencing and Its Applications. *Genomics, Proteomics & Bioinformatics* **2015**, *13*, 278–289, doi:10.1016/j.gpb.2015.08.002.
9. Kono, N.; Arakawa, K. Nanopore Sequencing: Review of Potential Applications in Functional Genomics. *Development, Growth & Differentiation* **2019**, *61*, 316–326, doi:10.1111/dgd.12608.
10. Foox, J.; Tighe, S.W.; Nicolet, C.M.; Zook, J.M.; Byrska-Bishop, M.; Clarke, W.E.; Khayat, M.M.; Mahmoud, M.; Laaguiby, P.K.; Herbert, Z.T.; et al. Performance Assessment of DNA Sequencing Platforms in the ABRF Next-Generation Sequencing Study. *Nat Biotechnol* **2021**, *39*, 1129–1140, doi:10.1038/s41587-021-01049-5.
11. Gardy, J.L.; Loman, N.J. Towards a Genomics-Informed, Real-Time, Global Pathogen Surveillance System. *Nat Rev Genet* **2018**, *19*, 9–20, doi:10.1038/nrg.2017.88.
12. Inzaule, S.C.; Tessema, S.K.; Kebede, Y.; Ogwell Ouma, A.E.; Nkengasong, J.N. Genomic-Informed Pathogen Surveillance in Africa: Opportunities and Challenges. *Lancet Infect Dis* **2021**, *21*, e281–e289, doi:10.1016/S1473-3099(20)30939-7.
13. Jacobsen, K.H.; Aguirre, A.A.; Bailey, C.L.; Baranova, A.V.; Crooks, A.T.; Croitoru, A.; Delamater, P.L.; Gupta, J.; Kehn-Hall, K.; Narayanan, A.; et al.

Lessons from the Ebola Outbreak: Action Items for Emerging Infectious Disease Preparedness and Response. *Ecohealth* **2016**, *13*, 200–212, doi:10.1007/s10393-016-1100-5.
14. Vinayagamoorthy, T.; Mulatz, K.; Hodkinson, R. Identification of the Severe Acute Respiratory Syndrome Coronavirus by Simultaneous Multigene DNA Sequencing. *J Clin Microbiol* **2004**, *42*, 3291–3294, doi:10.1128/JCM.42.7.3291-3294.2004.
15. Jacob Machado, D.; White, R.A.; Kofsky, J.; Janies, D.A. Fundamentals of Genomic Epidemiology, Lessons Learned from the Coronavirus Disease 2019 (COVID-19) Pandemic, and New Directions. *Antimicrob Steward Healthc Epidemiol* **2021**, *1*, e60, doi:10.1017/ash.2021.222.
16. Fogel, J.M.; Bonsall, D.; Cummings, V.; Bowden, R.; Golubchik, T.; de Cesare, M.; Wilson, E.A.; Gamble, T.; del Rio, C.; Batey, D.S.; et al. Performance of a High-Throughput next-Generation Sequencing Method for Analysis of HIV Drug Resistance and Viral Load. *J Antimicrob Chemother* **2020**, *75*, 3510–3516, doi:10.1093/jac/dkaa352.
17. FISHER, R.G.; SMITH, D.M.; MURRELL, B.; SLABBERT, R.; KIRBY, B.M.; EDSON, C.; COTTON, M.F.; HAUBRICH, R.H.; KOSAKOVSKY POND, S.L.; VAN ZYL, G.U. Next Generation Sequencing Improves Detection of Drug Resistance Mutations in Infants after PMTCT Failure. *J Clin Virol* **2015**, *62*, 48–53, doi:10.1016/j.jcv.2014.11.014.
18. Dohál, M.; Dvořáková, V.; Šperková, M.; Pinková, M.; Spitaleri, A.; Norman, A.; Cabibbe, A.M.; Rasmussen, E.M.; Porvazník, I.; Škereňová, M.; et al. Whole Genome Sequencing of Multidrug-Resistant Mycobacterium Tuberculosis Isolates Collected in the Czech Republic, 2005–2020. *Sci Rep* **2022**, *12*, 7149, doi:10.1038/s41598-022-11287-5.
19. Otte, A.; Marriott, A.C.; Dreier, C.; Dove, B.; Mooren, K.; Klingen, T.R.; Sauter, M.; Thompson, K.-A.; Bennett, A.; Klingel, K.; et al. Evolution of 2009 H1N1 Influenza Viruses during the Pandemic Correlates with Increased Viral Pathogenicity and Transmissibility in the Ferret Model. *Sci Rep* **2016**, *6*, 28583, doi:10.1038/srep28583.
20. Maes, E.F.; Diop, O.M.; Jorba, J.; Chavan, S.; Tangermann, R.H.; Wassilak, S.G.F. Surveillance Systems to Track Progress Toward Polio Eradication — Worldwide, 2015–2016. *MMWR Morb Mortal Wkly Rep* **2017**, *66*, 359–365, doi:10.15585/mmwr.mm6613a3.
21. Kurosaki, Y.; Martins, D.B.G.; Kimura, M.; Catena, A. dos S.; Borba, M.A.C.S.M.; Mattos, S. da S.; Abe, H.; Yoshikawa, R.; de Lima Filho, J.L.; Yasuda, J. Development and Evaluation of a Rapid Molecular Diagnostic Test for Zika Virus Infection by Reverse Transcription Loop-Mediated Isothermal Amplification. *Sci Rep* **2017**, *7*, 13503, doi:10.1038/s41598-017-13836-9.
22. Ren, S.-Y.; Wang, W.-B.; Gao, R.-D.; Zhou, A.-M. Omicron Variant (B.1.1.529) of SARS-CoV-2: Mutation, Infectivity, Transmission, and Vaccine Resistance. *World J Clin Cases* **2022**, *10*, 1–11, doi:10.12998/wjcc.v10.i1.1.
23. Iketani, S.; Liu, L.; Guo, Y.; Liu, L.; Chan, J.F.-W.; Huang, Y.; Wang, M.; Luo, Y.; Yu, J.; Chu, H.; et al. Antibody Evasion Properties of SARS-CoV-2 Omicron Sublineages. *Nature* **2022**, *604*, 553–556, doi:10.1038/s41586-022-04594-4.

24. Garcia-Beltran, W.F.; St. Denis, K.J.; Hoelzemer, A.; Lam, E.C.; Nitido, A.D.; Sheehan, M.L.; Berrios, C.; Ofoman, O.; Chang, C.C.; Hauser, B.M.; et al. mRNA-Based COVID-19 Vaccine Boosters Induce Neutralizing Immunity against SARS-CoV-2 Omicron Variant. *Cell* **2022**, *185*, 457-466.e4, doi:10.1016/j.cell.2021.12.033.
25. Cele, S.; Jackson, L.; Khoury, D.S.; Khan, K.; Moyo-Gwete, T.; Tegally, H.; San, J.E.; Cromer, D.; Scheepers, C.; Amoako, D.; et al. SARS-CoV-2 Omicron Has Extensive but Incomplete Escape of Pfizer BNT162b2 Elicited Neutralization and Requires ACE2 for Infection. *medRxiv* **2021**, 2021.12.08.21267417, doi:10.1101/2021.12.08.21267417.
26. Saxena, S.K.; Kumar, S.; Ansari, S.; Paweska, J.T.; Maurya, V.K.; Tripathi, A.K.; Abdel-Moneim, A.S. Characterization of the Novel SARS-CoV-2 Omicron (B.1.1.529) Variant of Concern and Its Global Perspective. *Journal of Medical Virology* **2022**, *94*, 1738–1744, doi:10.1002/jmv.27524.
27. Lusvarghi, S.; Pollett, S.D.; Neerukonda, S.N.; Wang, W.; Wang, R.; Vassell, R.; Epsi, N.J.; Fries, A.C.; Agan, B.K.; Lindholm, D.A.; et al. SARS-CoV-2 Omicron Neutralization by Therapeutic Antibodies, Convalescent Sera, and Post-mRNA Vaccine Booster. *bioRxiv* **2021**, 2021.12.22.473880, doi:10.1101/2021.12.22.473880.
28. Modes, M.E. Clinical Characteristics and Outcomes Among Adults Hospitalized with Laboratory-Confirmed SARS-CoV-2 Infection During Periods of B.1.617.2 (Delta) and B.1.1.529 (Omicron) Variant Predominance — One Hospital, California, July 15–September 23, 2021, and December 21, 2021–January 27, 2022. *MMWR Morb Mortal Wkly Rep* **2022**, *71*, doi:10.15585/mmwr.mm7106e2.
29. Wadford, D.A.; Baumrind, N.; Baylis, E.F.; Bell, J.M.; Bouchard, E.L.; Crumpler, M.; Foote, E.M.; Gilliam, S.; Glaser, C.A.; Hacker, J.K.; et al. Implementation of California COVIDNet – a Multi-Sector Collaboration for Statewide SARS-CoV-2 Genomic Surveillance. *Frontiers in Public Health* **2023**, *11*.
30. Pellett, P.E.; Mitra, S.; Holland, T.C. Basics of Virology. *Handb Clin Neurol* **2014**, *123*, 45–66, doi:10.1016/B978-0-444-53488-0.00002-X.
31. Ciuffi, A.; Rato, S.; Telenti, A. Single-Cell Genomics for Virology. *Viruses* **2016**, *8*, 123, doi:10.3390/v8050123.
32. Rato, S.; Golumbeanu, M.; Telenti, A.; Ciuffi, A. Exploring Viral Infection Using Single-Cell Sequencing. *Virus Research* **2017**, *239*, 55–68, doi:10.1016/j.virusres.2016.10.016.
33. Wylie, K.M.; Weinstock, G.M.; Storch, G.A. Virome Genomics: A Tool for Defining the Human Virome. *Curr Opin Microbiol* **2013**, *16*, 479–484, doi:10.1016/j.mib.2013.04.006.
34. QUIÑONES-MATEU, M.E.; AVILA, S.; REYES-TERAN, G.; MARTINEZ, M.A. Deep Sequencing: Becoming a Critical Tool in Clinical Virology. *J Clin Virol* **2014**, *61*, 9–19, doi:10.1016/j.jcv.2014.06.013.
35. Rascovan, N.; Duraisamy, R.; Desnues, C. Metagenomics and the Human Virome in Asymptomatic Individuals. *Annual Review of Microbiology* **2016**, *70*, 125–141, doi:10.1146/annurev-micro-102215-095431.
36. Pollara, J.; Khanal, S.; Edwards, R.W.; Hora, B.; Ferrari, G.; Haynes, B.F.; Bradley, T. Single-Cell Analysis of Immune Cell Transcriptome during HIV-1

Infection and Therapy. *BMC Immunology* **2022**, *23*, 48, doi:10.1186/s12865-022-00523-2.
37. Boldanova, T.; Suslov, A.; Heim, M.H.; Necsulea, A. Transcriptional Response to Hepatitis C Virus Infection and Interferon-alpha Treatment in the Human Liver. *EMBO Mol Med* **2017**, *9*, 816–834, doi:10.15252/emmm.201607006.
38. Liu, X.; Speranza, E.; Muñoz-Fontela, C.; Haldenby, S.; Rickett, N.Y.; Garcia-Dorival, I.; Fang, Y.; Hall, Y.; Zekeng, E.-G.; Lüdtke, A.; et al. Transcriptomic Signatures Differentiate Survival from Fatal Outcomes in Humans Infected with Ebola Virus. *Genome Biol* **2017**, *18*, 4, doi:10.1186/s13059-016-1137-3.
39. A Next Generation Sequencing (NGS) Approach to Influenza Vaccine Development.
40. Ghedin, E.; Sengamalay, N.A.; Shumway, M.; Zaborsky, J.; Feldblyum, T.; Subbu, V.; Spiro, D.J.; Sitz, J.; Koo, H.; Bolotov, P.; et al. Large-Scale Sequencing of Human Influenza Reveals the Dynamic Nature of Viral Genome Evolution. *Nature* **2005**, *437*, 1162–1166, doi:10.1038/nature04239.
41. Ojosnegros, S.; Beerenwinkel, N. Models of RNA Virus Evolution and Their Roles in Vaccine Design. *Immunome Research* **2010**, *6*, S5, doi:10.1186/1745-7580-6-S2-S5.
42. Gutiérrez, P.A.; Elena, S.F. Single-Cell RNA-Sequencing Data Analysis Reveals a Highly Correlated Triphasic Transcriptional Response to SARS-CoV-2 Infection. *Commun Biol* **2022**, *5*, 1–13, doi:10.1038/s42003-022-04253-4.
43. Medaglia, C.; Kolpakov, I.; Zwygart, A.C.-A.; Zhu, Y.; Constant, S.; Huang, S.; Cagno, V.; Dermitzakis, E.T.; Stellacci, F.; Xenarios, I.; et al. An Anti-Influenza Combined Therapy Assessed by Single Cell RNA-Sequencing. *Commun Biol* **2022**, *5*, 1–14, doi:10.1038/s42003-022-04013-4.
44. O'Neill, M.B.; Quach, H.; Pothlichet, J.; Aquino, Y.; Bisiaux, A.; Zidane, N.; Deschamps, M.; Libri, V.; Hasan, M.; Zhang, S.-Y.; et al. Single-Cell and Bulk RNA-Sequencing Reveal Differences in Monocyte Susceptibility to Influenza A Virus Infection Between Africans and Europeans. *Frontiers in Immunology* **2021**, *12*.
45. Brown, D.; Altermatt, M.; Dobreva, T.; Chen, S.; Wang, A.; Thomson, M.; Gradinaru, V. Deep Parallel Characterization of AAV Tropism and AAV-Mediated Transcriptional Changes via Single-Cell RNA Sequencing. *Frontiers in Immunology* **2021**, *12*.
46. Zheng, M. Cellular Tropism of SARS-CoV-2 across Human Tissues and Age-Related Expression of ACE2 and TMPRSS2 in Immune-Inflammatory Stromal Cells. *Aging Dis* **2021**, *12*, 718–725, doi:10.14336/AD.2021.0429.
47. Wyler, E.; Franke, V.; Menegatti, J.; Kocks, C.; Boltengagen, A.; Praktiknjo, S.; Walch-Rückheim, B.; Bosse, J.; Rajewsky, N.; Grässer, F.; et al. Single-Cell RNA-Sequencing of Herpes Simplex Virus 1-Infected Cells Connects NRF2 Activation to an Antiviral Program. *Nat Commun* **2019**, *10*, 4878, doi:10.1038/s41467-019-12894-z.
48. Chang, J.-T.; Liu, L.-B.; Wang, P.-G.; An, J. Single-Cell RNA Sequencing to Understand Host-Virus Interactions. *Virologica Sinica* **2023**, doi:10.1016/j.virs.2023.11.009.

49. Cao, Q.; Wu, S.; Xiao, C.; Chen, S.; Chi, X.; Cui, X.; Tang, H.; Su, W.; Zheng, Y.; Zhong, J.; et al. Integrated Single-Cell Analysis Revealed Immune Dynamics during Ad5-nCoV Immunization. *Cell Discov* **2021**, *7*, 1–17, doi:10.1038/s41421-021-00300-2.
50. Van de Sande, B.; Lee, J.S.; Mutasa-Gottgens, E.; Naughton, B.; Bacon, W.; Manning, J.; Wang, Y.; Pollard, J.; Mendez, M.; Hill, J.; et al. Applications of Single-Cell RNA Sequencing in Drug Discovery and Development. *Nat Rev Drug Discov* **2023**, *22*, 496–520, doi:10.1038/s41573-023-00688-4.
51. Iwasaki, A.; Pillai, P.S. Innate Immunity to Influenza Virus Infection. *Nat Rev Immunol* **2014**, *14*, 315–328, doi:10.1038/nri3665.
52. Della Chiesa, M.; De Maria, A.; Muccio, L.; Bozzano, F.; Sivori, S.; Moretta, L. Human NK Cells and Herpesviruses: Mechanisms of Recognition, Response and Adaptation. *Frontiers in Microbiology* **2019**, *10*.
53. Bertoletti, A.; Ferrari, C. Adaptive Immunity in HBV Infection. *Journal of Hepatology* **2016**, *64*, S71–S83, doi:10.1016/j.jhep.2016.01.026.
54. Letvin, N.L. Progress and Obstacles in the Development of an AIDS Vaccine. *Nat Rev Immunol* **2006**, *6*, 930–939, doi:10.1038/nri1959.
55. Narisawa-Saito, M.; Kiyono, T. Basic Mechanisms of High-Risk Human Papillomavirus-Induced Carcinogenesis: Roles of E6 and E7 Proteins. *Cancer Science* **2007**, *98*, 1505–1511, doi:10.1111/j.1349-7006.2007.00546.x.
56. Lee, N.; Hurt, A.C. Neuraminidase Inhibitor Resistance in Influenza: A Clinical Perspective. *Current Opinion in Infectious Diseases* **2018**, *31*, 520, doi:10.1097/QCO.0000000000000498.
57. Hoon, M.; Okawa, H.; Santina, L.D.; Wong, R.O.L. Functional Architecture of the Retina: Development and Disease. *Prog Retin Eye Res* **2014**, *42*, 44–84, doi:10.1016/j.preteyeres.2014.06.003.
58. Sobhy, H. A Comparative Review of Viral Entry and Attachment during Large and Giant dsDNA Virus Infections. *Arch Virol* **2017**, *162*, 3567–3585, doi:10.1007/s00705-017-3497-8.
59. Bodaghi, B.; Slobbe–vanDrunen, M.E.P.; Topilko, A.; Perret, E.; Vossen, R.C.R.M.; van Dam–Mieras, M.C.E.; Zipeto, D.; Virelizier, J.-L.; LeHoang, P.; Bruggeman, C.A.; et al. Entry of Human Cytomegalovirus into Retinal Pigment Epithelial and Endothelial Cells by Endocytosis. *Investigative Ophthalmology & Visual Science* **1999**, *40*, 2598–2607.
60. Shukla, S.Y.; Singh, Y.K.; Shukla, D. Role of Nectin-1, HVEM, and PILR-α in HSV-2 Entry into Human Retinal Pigment Epithelial Cells. *Investigative Ophthalmology & Visual Science* **2009**, *50*, 2878–2887, doi:10.1167/iovs.08-2981.
61. Gao, J.; Guo, Z.; Li, W.; Zhang, X.; Zhang, X.-E.; Cui, Z. Ebola Virus Disrupts the Inner Blood-Retinal Barrier by Induction of Vascular Endothelial Growth Factor in Pericytes. *PLOS Pathogens* **2023**, *19*, e1011077, doi:10.1371/journal.ppat.1011077.
62. Muthiah, M.N.; Michaelides, M.; Child, C.S.; Mitchell, S.M. Acute Retinal Necrosis: A National Population-based Study to Assess the Incidence, Methods of Diagnosis, Treatment Strategies and Outcomes in the UK. *Br J Ophthalmol* **2007**, *91*, 1452–1455, doi:10.1136/bjo.2007.114884.

63. Viral Retinitis: Diagnosis and Management in the Era of Biologic Immunosuppression: A Review - Wu - 2019 - Clinical & Experimental Ophthalmology - Wiley Online Library Available online: https://onlinelibrary.wiley.com/doi/10.1111/ceo.13500 (accessed on 11 January 2024).
64. Guo, H.; Koehler, H.S.; Dix, R.D.; Mocarski, E.S. Programmed Cell Death-Dependent Host Defense in Ocular Herpes Simplex Virus Infection. *Front Microbiol* **2022**, *13*, 869064, doi:10.3389/fmicb.2022.869064.
65. Svozílková, P.; Říhová, E.; Diblík, P.; Kuthan, P.; Kovařík, Z.; Kalvodová, B. Varicella Zoster Virus Acute Retinal Necrosis Following Eye Contusion: Case Report. *Virology Journal* **2005**, *2*, 77, doi:10.1186/1743-422X-2-77.
66. Freitas, D.A.; Souza-Santos, R.; Carvalho, L.M.A.; Barros, W.B.; Neves, L.M.; Brasil, P.; Wakimoto, M.D. Congenital Zika Syndrome: A Systematic Review. *PLoS One* **2020**, *15*, e0242367, doi:10.1371/journal.pone.0242367.
67. Costa, C.B. da C.; Freitas, D. Ocular Findings of Congenital Zika Virus Infection with Microcephaly. *Int Ophthalmol* **2022**, *42*, 3117–3127, doi:10.1007/s10792-022-02311-8.
68. Singh, S.; Farr, D.; Kumar, A. Ocular Manifestations of Emerging Flaviviruses and the Blood-Retinal Barrier. *Viruses* **2018**, *10*, 530, doi:10.3390/v10100530.
69. Labib, B.A.; Chigbu, D.I. Pathogenesis and Manifestations of Zika Virus-Associated Ocular Diseases. *Trop Med Infect Dis* **2022**, *7*, 106, doi:10.3390/tropicalmed7060106.
70. Duarte, L.F.; Farías, M.A.; Álvarez, D.M.; Bueno, S.M.; Riedel, C.A.; González, P.A. Herpes Simplex Virus Type 1 Infection of the Central Nervous System: Insights Into Proposed Interrelationships With Neurodegenerative Disorders. *Frontiers in Cellular Neuroscience* **2019**, *13*.
71. Zhu, S.; Viejo-Borbolla, A. Pathogenesis and Virulence of Herpes Simplex Virus. *Virulence 12*, 2670–2702, doi:10.1080/21505594.2021.1982373.
72. Fan, S.; Yoo, J.H.; Park, G.; Yeh, S.; Conrady, C.D. Type I Interferon Signaling Is Critical During the Innate Immune Response to HSV-1 Retinal Infection. *Invest Ophthalmol Vis Sci* **2022**, *63*, 28, doi:10.1167/iovs.63.13.28.
73. Wilcox, D.R.; Folmsbee, S.S.; Muller, W.J.; Longnecker, R. The Type I Interferon Response Determines Differences in Choroid Plexus Susceptibility between Newborns and Adults in Herpes Simplex Virus Encephalitis. *mBio* **2016**, *7*, e00437-16, doi:10.1128/mBio.00437-16.
74. Wang, J.P.; Bowen, G.N.; Zhou, S.; Cerny, A.; Zacharia, A.; Knipe, D.M.; Finberg, R.W.; Kurt-Jones, E.A. Role of Specific Innate Immune Responses in Herpes Simplex Virus Infection of the Central Nervous System. *J Virol* **2012**, *86*, 2273–2281, doi:10.1128/JVI.06010-11.
75. Singh, H.P.; Wang, S.; Stachelek, K.; Lee, S.; Reid, M.W.; Thornton, M.E.; Craft, C.M.; Grubbs, B.H.; Cobrinik, D. Developmental Stage-Specific Proliferation and Retinoblastoma Genesis in RB-Deficient Human but Not Mouse Cone Precursors. *Proc Natl Acad Sci U S A* **2018**, *115*, E9391–E9400, doi:10.1073/pnas.1808903115.
76. Zhang, X.; Wang, W.; Jin, Z.-B. Retinal Organoids as Models for Development and Diseases. *Cell Regen* **2021**, *10*, 33, doi:10.1186/s13619-021-00097-1.

77. Menuchin-Lasowski, Y.; Schreiber, A.; Lecanda, A.; Mecate-Zambrano, A.; Brunotte, L.; Psathaki, O.E.; Ludwig, S.; Rauen, T.; Schöler, H.R. SARS-CoV-2 Infects and Replicates in Photoreceptor and Retinal Ganglion Cells of Human Retinal Organoids. *Stem Cell Reports* **2022**, *17*, 789–803, doi:10.1016/j.stemcr.2022.02.015.
78. Sudharsan, R.; Beiting, D.P.; Aguirre, G.D.; Beltran, W.A. Involvement of Innate Immune System in Late Stages of Inherited Photoreceptor Degeneration. *Sci Rep* **2017**, *7*, 17897, doi:10.1038/s41598-017-18236-7.
79. Völkner, M.; Wagner, F.; Kurth, T.; Sykes, A.M.; Del Toro Runzer, C.; Ebner, L.J.A.; Kavak, C.; Alexaki, V.I.; Cimalla, P.; Mehner, M.; et al. Modeling Inducible Neuropathologies of the Retina with Differential Phenotypes in Organoids. *Frontiers in Cellular Neuroscience* **2023**, *17*.
80. Kruczek, K.; Swaroop, A. Pluripotent Stem Cell-Derived Retinal Organoids for Disease Modeling and Development of Therapies. *Stem Cells* **2020**, *38*, 1206–1215, doi:10.1002/stem.3239.
81. Zhao, H.; Yan, F. Retinal Organoids: A Next-Generation Platform for High-Throughput Drug Discovery. *Stem Cell Rev and Rep* **2023**, doi:10.1007/s12015-023-10661-8.
82. Thomas, S. Status of COVID-19 Pandemic Before the Administration of Vaccine. *Methods Mol Biol* **2022**, *2410*, 93–108, doi:10.1007/978-1-0716-1884-4_4.
83. Zhao, Y.; Huang, J.; Zhang, L.; Chen, S.; Gao, J.; Jiao, H. The Global Transmission of New Coronavirus Variants. *Environ Res* **2022**, *206*, 112240, doi:10.1016/j.envres.2021.112240.
84. Eyre, D.W.; Taylor, D.; Purver, M.; Chapman, D.; Fowler, T.; Pouwels, K.B.; Walker, A.S.; Peto, T.E.A. Effect of Covid-19 Vaccination on Transmission of Alpha and Delta Variants. *N Engl J Med* **2022**, *386*, 744–756, doi:10.1056/NEJMoa2116597.
85. Gobeil, S.M.-C.; Janowska, K.; McDowell, S.; Mansouri, K.; Parks, R.; Stalls, V.; Kopp, M.F.; Manne, K.; Li, D.; Wiehe, K.; et al. Effect of Natural Mutations of SARS-CoV-2 on Spike Structure, Conformation and Antigenicity. *Science* **2021**, *373*, eabi6226, doi:10.1126/science.abi6226.
86. Escalera, A.; Gonzalez-Reiche, A.S.; Aslam, S.; Mena, I.; Laporte, M.; Pearl, R.L.; Fossati, A.; Rathnasinghe, R.; Alshammary, H.; van de Guchte, A.; et al. Mutations in SARS-CoV-2 Variants of Concern Link to Increased Spike Cleavage and Virus Transmission. *Cell Host Microbe* **2022**, *30*, 373-387.e7, doi:10.1016/j.chom.2022.01.006.
87. Li, Q.; Wu, J.; Nie, J.; Zhang, L.; Hao, H.; Liu, S.; Zhao, C.; Zhang, Q.; Liu, H.; Nie, L.; et al. The Impact of Mutations in SARS-CoV-2 Spike on Viral Infectivity and Antigenicity. *Cell* **2020**, *182*, 1284-1294.e9, doi:10.1016/j.cell.2020.07.012.
88. Tracking SARS-CoV-2 Variants Available online: https://www.who.int/activities/tracking-SARS-CoV-2-variants (accessed on 19 May 2022).
89. du Plessis, L.; McCrone, J.T.; Zarebski, A.E.; Hill, V.; Ruis, C.; Gutierrez, B.; Raghwani, J.; Ashworth, J.; Colquhoun, R.; Connor, T.R.; et al. Establishment

and Lineage Dynamics of the SARS-CoV-2 Epidemic in the UK. *Science* **2021**, eabf2946, doi:10.1126/science.abf2946.
90. Mercer, T.R.; Salit, M. Testing at Scale during the COVID-19 Pandemic. *Nat Rev Genet* **2021**, 1–12, doi:10.1038/s41576-021-00360-w.
91. Sam, I.; Chong, Y.M.; Abdullah, A.; Fu, J.Y.L.; Hasan, M.S.; Jamaluddin, F.H.; Kamarulzaman, A.; Lim, K.K.; Mohd Nor, M.A.; Pang, Y.K.; et al. Changing Predominant SARS-CoV-2 Lineages Drives Successive COVID-19 Waves in Malaysia, February 2020 to March 2021. *J Med Virol* **2021**, 10.1002/jmv.27441, doi:10.1002/jmv.27441.
92. Oude Munnink, B.B.; Worp, N.; Nieuwenhuijse, D.F.; Sikkema, R.S.; Haagmans, B.; Fouchier, R.A.M.; Koopmans, M. The next Phase of SARS-CoV-2 Surveillance: Real-Time Molecular Epidemiology. *Nat Med* **2021**, *27*, 1518–1524, doi:10.1038/s41591-021-01472-w.
93. Thakur, V.; Ratho, R.K. OMICRON (B.1.1.529): A New SARS-CoV-2 Variant of Concern Mounting Worldwide Fear. *Journal of Medical Virology* **2022**, *94*, 1821–1824, doi:10.1002/jmv.27541.
94. Classification of Omicron (B.1.1.529): SARS-CoV-2 Variant of Concern Available online: https://www.who.int/news/item/26-11-2021-classification-of-omicron-(b.1.1.529)-sars-cov-2-variant-of-concern (accessed on 19 May 2022).
95. Outbreak.Info Available online: https://outbreak.info/ (accessed on 23 May 2022).
96. Kumar, S.; Karuppanan, K.; Subramaniam, G. Omicron (BA.1) and Sub-Variants (BA.1, BA.2 and BA.3) of SARS-CoV-2 Spike Infectivity and Pathogenicity: A Comparative Sequence and Structural-Based Computational Assessment 2022, 2022.02.11.480029.
97. Chen, J.; Wei, G.-W. Omicron BA.2 (B.1.1.529.2): High Potential to Becoming the next Dominating Variant. *ArXiv* **2022**, arXiv:2202.05031v1.
98. Chen, J.; Wang, R.; Gilby, N.B.; Wei, G.-W. Omicron Variant (B.1.1.529): Infectivity, Vaccine Breakthrough, and Antibody Resistance. *J Chem Inf Model* **2022**, acs.jcim.1c01451, doi:10.1021/acs.jcim.1c01451.
99. Li, J.; Gao, Z.; Chen, J.; Cheng, R.; Niu, J.; Zhang, J.; Yang, Y.; Yuan, X.; Xia, J.; Mao, G.; et al. Development of a Panel of Three Multiplex Allele-Specific qRT-PCR Assays for Quick Differentiation of Recombinant Variants and Omicron Subvariants of SARS-CoV-2. *Frontiers in Cellular and Infection Microbiology* **2022**, *12*.
100. Ippoliti, C.; De Maio, F.; Santarelli, G.; Marchetti, S.; Vella, A.; Santangelo, R.; Sanguinetti, M.; Posteraro, B. Rapid Detection of the Omicron (B.1.1.529) SARS-CoV-2 Variant Using a COVID-19 Diagnostic PCR Assay. *Microbiology Spectrum* **2022**, *10*, e00990-22, doi:10.1128/spectrum.00990-22.
101. Corbisier, P.; Petrillo, M.; Marchini, A.; Querci, M.; Buttinger, G.; Bekliz, M.; Spiess, K.; Polacek, C.; Fomsgaard, A.; Van den Eede, G. A Qualitative RT-PCR Assay for the Specific Identification of the SARS-CoV-2 B.1.1.529 (Omicron) Variant of Concern. *Journal of Clinical Virology* **2022**, *152*, 105191, doi:10.1016/j.jcv.2022.105191.
102. Mills, M.G.; Hajian, P.; Bakhash, S.M.; Xie, H.; Mantzke, D.; Zhu, H.; Perchetti, G.A.; Huang, M.-L.; Pepper, G.; Jerome, K.R.; et al. Rapid and

Accurate Identification of SARS-CoV-2 Omicron Variants Using Droplet Digital PCR (RT-ddPCR). *Journal of Clinical Virology* **2022**, *154*, 105218, doi:10.1016/j.jcv.2022.105218.
103. Koshikawa, T.; Miyoshi, H. High-Resolution Melting Analysis to Discriminate between the SARS-CoV-2 Omicron Variants BA.1 and BA.2. *Biochemistry and Biophysics Reports* **2022**, *31*, 101306, doi:10.1016/j.bbrep.2022.101306.
104. Aoki, A.; Adachi, H.; Mori, Y.; Ito, M.; Sato, K.; Okuda, K.; Sakakibara, T.; Okamoto, Y.; Jinno, H. Discrimination of SARS-CoV-2 Omicron Sub-Lineages BA.1 and BA.2 Using a High-Resolution Melting-Based Assay: A Pilot Study 2022, 2022.04.11.487970.
105. Yan, T.; Xu, Y.; Zheng, R.; Zeng, X.; Chen, Z.; Lin, S.; Xia, Z.; Liao, Y.; Zhang, Y.; Li, Q. Accessible and Adaptable Multiplexed Real-Time PCR Approaches to Identify SARS-CoV-2 Variants of Concern. *Microbiology Spectrum* **2022**, *10*, e03222-22, doi:10.1128/spectrum.03222-22.
106. Clark, A.E.; Wang, Z.; Ostman, E.; Zheng, H.; Yao, H.; Cantarel, B.; Kanchwala, M.; Xing, C.; Chen, L.; Irwin, P.; et al. Multiplex Fragment Analysis for Flexible Detection of All SARS-CoV-2 Variants of Concern. *Clin Chem* **2022**, *68*, 1042–1052, doi:10.1093/clinchem/hvac081.
107. Hernandez, M.M.; Banu, R.; Shrestha, P.; Gonzalez-Reiche, A.S.; van de Guchte, A.; Farrugia, K.; Sebra, R.; Mount Sinai PSP Study Group; Gitman, M.R.; Nowak, M.D.; et al. A Robust, Highly Multiplexed Mass Spectrometry Assay to Identify SARS-CoV-2 Variants. *Microbiology Spectrum* **2022**, *10*, e01736-22, doi:10.1128/spectrum.01736-22.
108. Gerdol, M.; Dishnica, K.; Giorgetti, A. Emergence of a Recurrent Insertion in the N-Terminal Domain of the SARS-CoV-2 Spike Glycoprotein. *Virus Research* **2022**, *310*, 198674, doi:10.1016/j.virusres.2022.198674.
109. CoVariants: 21K (Omicron) Available online: https://covariants.org/variants/21K.Omicron (accessed on 23 May 2022).
110. CoVariants: 21L (Omicron) Available online: https://covariants.org/variants/21L.Omicron (accessed on 23 May 2022).
111. Borillo, G.A.; Kagan, R.M.; Marlowe, E.M. Rapid and Accurate Identification of SARS-CoV-2 Variants Using Real Time PCR Assays. *Frontiers in Cellular and Infection Microbiology* **2022**, *12*.
112. Vega-Magaña, N.; Sánchez-Sánchez, R.; Hernández-Bello, J.; Venancio-Landeros, A.A.; Peña-Rodríguez, M.; Vega-Zepeda, R.A.; Galindo-Ornelas, B.; Díaz-Sánchez, M.; García-Chagollán, M.; Macedo-Ojeda, G.; et al. RT-qPCR Assays for Rapid Detection of the N501Y, 69-70del, K417N, and E484K SARS-CoV-2 Mutations: A Screening Strategy to Identify Variants With Clinical Impact. *Frontiers in Cellular and Infection Microbiology* **2021**, *11*.
113. Oh, C.; Sashittal, P.; Zhou, A.; Wang, L.; El-Kebir, M.; Nguyen, T.H. Design of SARS-CoV-2 Variant-Specific PCR Assays Considering Regional and Temporal Characteristics. *Applied and Environmental Microbiology* **2022**, *88*, e02289-21, doi:10.1128/aem.02289-21.
114. Martinez, D.; Miyasaki, T.; Chow, E. UCSF CAT COVID-19 Tailed 275bp v3 ARTIC Protocol V1. *protocols.io* **2021**.

115. Hadfield, J.; Megill, C.; Bell, S.M.; Huddleston, J.; Potter, B.; Callender, C.; Sagulenko, P.; Bedford, T.; Neher, R.A. Nextstrain: Real-Time Tracking of Pathogen Evolution. *Bioinformatics* **2018**, *34*, 4121–4123, doi:10.1093/bioinformatics/bty407.
116. Yu, G.; Smith, D.K.; Zhu, H.; Guan, Y.; Lam, T.T.-Y. Ggtree: An r Package for Visualization and Annotation of Phylogenetic Trees with Their Covariates and Other Associated Data. *Methods in Ecology and Evolution* **2017**, *8*, 28–36, doi:10.1111/2041-210X.12628.
117. Santa Barbara County Community Data Dashboard Available online: https://sbcphd.maps.arcgis.com/apps/MapSeries/index.html?appid=55b1e071669c46c1b939126e1c265bae (accessed on 26 May 2022).
118. Paul, P.; France, A.M.; Aoki, Y.; Batra, D.; Biggerstaff, M.; Dugan, V.; Galloway, S.; Hall, A.J.; Johansson, M.A.; Kondor, R.J.; et al. Genomic Surveillance for SARS-CoV-2 Variants Circulating in the United States, December 2020–May 2021. *MMWR Morb. Mortal. Wkly. Rep.* **2021**, *70*, 846–850, doi:10.15585/mmwr.mm7023a3.
119. Cao, Y.; Yisimayi, A.; Jian, F.; Song, W.; Xiao, T.; Wang, L.; Du, S.; Wang, J.; Li, Q.; Chen, X.; et al. BA.2.12.1, BA.4 and BA.5 Escape Antibodies Elicited by Omicron Infection. *Nature* **2022**, *608*, 593–602, doi:10.1038/s41586-022-04980-y.
120. Ventura, C.V.; Maia, M.; Travassos, S.B.; Martins, T.T.; Patriota, F.; Nunes, M.E.; Agra, C.; Torres, V.L.; van der Linden, V.; Ramos, R.C.; et al. Risk Factors Associated With the Ophthalmoscopic Findings Identified in Infants With Presumed Zika Virus Congenital Infection. *JAMA Ophthalmol* **2016**, *134*, 912–918, doi:10.1001/jamaophthalmol.2016.1784.
121. de Paula Freitas, B.; de Oliveira Dias, J.R.; Prazeres, J.; Sacramento, G.A.; Ko, A.I.; Maia, M.; Belfort, R. Ocular Findings in Infants With Microcephaly Associated With Presumed Zika Virus Congenital Infection in Salvador, Brazil. *JAMA Ophthalmol* **2016**, *134*, 529–535, doi:10.1001/jamaophthalmol.2016.0267.
122. Francis, P.J.; Jackson, H.; Stanford, M.R.; Graham, E.M. Inflammatory Optic Neuropathy as the Presenting Feature of Herpes Simplex Acute Retinal Necrosis. *Br J Ophthalmol* **2003**, *87*, 512–514.
123. Topp, K.S.; Bisla, K.; Saks, N.D.; Lavail, J.H. Centripetal Transport of Herpes Simplex Virus in Human Retinal Pigment Epithelial Cells in Vitro. *Neuroscience* **1996**, *71*, 1133–1144, doi:10.1016/0306-4522(95)00497-1.
124. Zhong, X.; Gutierrez, C.; Xue, T.; Hampton, C.; Vergara, M.N.; Cao, L.-H.; Peters, A.; Park, T.S.; Zambidis, E.T.; Meyer, J.S.; et al. Generation of Three-Dimensional Retinal Tissue with Functional Photoreceptors from Human iPSCs. *Nat Commun* **2014**, *5*, 4047, doi:10.1038/ncomms5047.
125. Sridhar, A.; Hoshino, A.; Finkbeiner, C.R.; Chitsazan, A.; Dai, L.; Haugan, A.K.; Eschenbacher, K.M.; Jackson, D.L.; Trapnell, C.; Bermingham-McDonogh, O.; et al. Single-Cell Transcriptomic Comparison of Human Fetal Retina, hPSC-Derived Retinal Organoids, and Long-Term Retinal Cultures. *Cell Rep* **2020**, *30*, 1644-1659.e4, doi:10.1016/j.celrep.2020.01.007.

126. Collin, J.; Queen, R.; Zerti, D.; Dorgau, B.; Hussain, R.; Coxhead, J.; Cockell, S.; Lako, M. Deconstructing Retinal Organoids: Single Cell RNA-Seq Reveals the Cellular Components of Human Pluripotent Stem Cell-Derived Retina. *Stem Cells* **2019**, *37*, 593–598, doi:10.1002/stem.2963.
127. Kim, S.; Lowe, A.; Dharmat, R.; Lee, S.; Owen, L.A.; Wang, J.; Shakoor, A.; Li, Y.; Morgan, D.J.; Hejazi, A.A.; et al. Generation, Transcriptome Profiling, and Functional Validation of Cone-Rich Human Retinal Organoids. *Proc Natl Acad Sci U S A* **2019**, *116*, 10824–10833, doi:10.1073/pnas.1901572116.
128. Liang, Q.; Dharmat, R.; Owen, L.; Shakoor, A.; Li, Y.; Kim, S.; Vitale, A.; Kim, I.; Morgan, D.; Liang, S.; et al. Single-Nuclei RNA-Seq on Human Retinal Tissue Provides Improved Transcriptome Profiling. *Nat Commun* **2019**, *10*, 5743, doi:10.1038/s41467-019-12917-9.
129. Zhou, Y.; Zhou, B.; Pache, L.; Chang, M.; Khodabakhshi, A.H.; Tanaseichuk, O.; Benner, C.; Chanda, S.K. Metascape Provides a Biologist-Oriented Resource for the Analysis of Systems-Level Datasets. *Nat Commun* **2019**, *10*, 1523, doi:10.1038/s41467-019-09234-6.
130. Zheng, G.X.Y.; Terry, J.M.; Belgrader, P.; Ryvkin, P.; Bent, Z.W.; Wilson, R.; Ziraldo, S.B.; Wheeler, T.D.; McDermott, G.P.; Zhu, J.; et al. Massively Parallel Digital Transcriptional Profiling of Single Cells. *Nat Commun* **2017**, *8*, 14049, doi:10.1038/ncomms14049.
131. McGinnis, C.S.; Murrow, L.M.; Gartner, Z.J. DoubletFinder: Doublet Detection in Single-Cell RNA Sequencing Data Using Artificial Nearest Neighbors. *Cell Systems* **2019**, *8*, 329-337.e4, doi:10.1016/j.cels.2019.03.003.
132. Butler, A.; Hoffman, P.; Smibert, P.; Papalexi, E.; Satija, R. Integrating Single-Cell Transcriptomic Data across Different Conditions, Technologies, and Species. *Nat Biotechnol* **2018**, *36*, 411–420, doi:10.1038/nbt.4096.
133. Blighe, K. Kevinblighe/EnhancedVolcano 2024.
134. Qiu, X.; Mao, Q.; Tang, Y.; Wang, L.; Chawla, R.; Pliner, H.A.; Trapnell, C. Reversed Graph Embedding Resolves Complex Single-Cell Trajectories. *Nat Methods* **2017**, *14*, 979–982, doi:10.1038/nmeth.4402.
135. Silverman, S.M.; Wong, W.T. Microglia in the Retina: Roles in Development, Maturity, and Disease. *Annu Rev Vis Sci* **2018**, *4*, 45–77, doi:10.1146/annurev-vision-091517-034425.
136. Chichagova, V.; Georgiou, M.; Carter, M.; Dorgau, B.; Hilgen, G.; Collin, J.; Queen, R.; Chung, G.; Ajeian, J.; Moya-Molina, M.; et al. Incorporating Microglia-like Cells in Human Induced Pluripotent Stem Cell-derived Retinal Organoids. *J Cell Mol Med* **2023**, *27*, 435–445, doi:10.1111/jcmm.17670.
137. Xu, R.; Boreland, A.J.; Li, X.; Erickson, C.; Jin, M.; Atkins, C.; Pang, Z.P.; Daniels, B.P.; Jiang, P. Developing Human Pluripotent Stem Cell-Based Cerebral Organoids with a Controllable Microglia Ratio for Modeling Brain Development and Pathology. *Stem Cell Reports* **2021**, *16*, 1923–1937, doi:10.1016/j.stemcr.2021.06.011.